Variscan orogeny in Corsica: new structural and geochronological insights, and its place in the Variscan geodynamic framework

Michel Faure, Philippe Rossi, Julien Gaché, Jérémie Melleton, Dirk Frei, Xian-Hua Li, Wei Lin

Variscan orogeny in Corsica: New structural and geochronological insights, and its place in the Variscan geodynamic framework

Michel Faure[1], Philippe Rossi[2, 3], Julien Gaché[1], Jérémie Melleton[1, 2], Dirk Frei[4], Xianhua Li[5], Wei Lin[5]

1: 1: Institut des Sciences de la Terre d'Orléans, UMR CNRS 7327, Université d'Orléans, 1A rue de la Férollerie, 45067 Orléans Cedex 2, France (michel.faure@univ-orleans.fr)

2 : BRGM, Av. Claude-Guillemin, BP 36009, 45060 Orléans Cedex 2, France

3: U Mercatu, Lama, 20218 Ponte Leccia.

4: Stellenbosch University, Department of Earth Sciences, Private Bag X1, Matieland, 7602, South Africa

5: State Key Laboratory of Lithospheric Evolution, Institute of Geology and Geophysics, Chinese Academy of Sciences, Beijing, China

Abstract

In Western Corsica, remnants of pre-batholitic lithological and metamorphic assemblages are preserved as km-scale septa enclosed within Lower Carboniferous to Early Permian plutons. Two groups of septa were recognized, 1) the Argentella and Agriates-Tenda fragments correspond to Neoproterozoic rocks deformed and metamorphosed during the Cadomian-Panafrican orogeny, and 2) the Zicavo, Porto Vecchio, Solenzara-Fautea, Belgodère, Topiti, and Vignola fragments consist of Variscan metamorphic rocks. The lithological content and the main ductile deformation events for each septum are presented. In the Zicavo, Porto

Vecchio, and Topiti septa, a top-to-the-SW ductile shearing (D1 event) coeval with an amphibolite facies metamorphism, is responsible for crustal thickening at ca 360 Ma. This main event was preceded by eclogite- and granulite-facies metamorphic events preserved as restites within migmatites dated at ca 345-330 Ma. A top-to-the-SE ductile shearing (D2 event), coeval with the crustal melting accommodated the exhumation of the D1 event. In contrast, the Belgodère segment is peculiar as it exhibits a top-to-the-east vergence, although retrogressed high-pressure rocks are also recognized. The pre-Permian fragments are arranged in four NW-SE striking stripes that define a SW-NE zoning with: i) a Western domain in Topiti, Vignola, Zicavo, Porto Vecchio, and Solenzara-Fautea, ii) a Neoproterozoic basement with its unconformable Early Paleozoic sedimentary cover in Argentella, iii) an Eastern metamorphic domain in Belgodère, iv) another Neoproterozoic basement with its Upper Paleozoic sedimentary cover in Agriates-Tenda. The Argentella basement is separated from the Western and Eastern domains by two sutures: S1 and S2. The Variscan Corsica represents the eastern part of the Sardinia-Corsica-Maures segment. The comparison of this segment with other Variscan domains allows us to propose some possible correlations. We argue that the Western domain, Argentella, Belgodère, and Agriates-Tenda domains can be compared with the southern Variscan belt exposed in French Massif Central-southern Massif Armoricain, Armorica microblock, Léon block, respectively.

Key words Variscan orogeny; Corsica; Synmetamorphic deformation; U-Th-Pb chemical dating; Crustal melting; Microcontinent collision; Armorica; Mid German Crystalline Rise

Introduction

The Paleozoic Variscan belt forms the backbone of Meso-Europa that develops from Southern Portugal to Poland. In spite of regional variations, a general picture of the present architecture of the chain, and its geodynamic evolution is now documented for the entire belt (e.g. Matte 1986; Franke 2000; Martínez Catalán et al. 2009; Ballèvre et al. 2009; Faure et al. 2005, 2009a; Schulmann et al. 2009). The Variscan belt also represents the basement of the Cenozoic Alpine and Pyrenean orogens in which it is exposed in the Crystalline Massifs and Axial zone, respectively. In the Western Mediterranean region, the Variscan basement is exposed in Corsica, Sardinia, Sicily islands, and in Calabria and Kabylia massifs. Due to the long lasting, and complex, geological history, namely Mesozoic rifting, Eocene Alpine orogeny, Oligocene-Miocene rifting, the geological correlations between these different elements, and the place of the Mediterranean massifs within the Variscan belt remain controversial (e.g. Carmignani et al. 1994; Elter et al. 1990; Matte et al. 2001; Corsini and Rolland 2009; Rossi et al. 2009).

This paper aims to present new structural and geochronological data of the pre-Permian rocks of Corsica, and to propose a possible tectonic interpretation of this Variscan segment consistent with the well documented Massif Armoricain and Massif Central of continental Europe.

Geological setting of the Variscan belt in Corsica

In Corsica, the Paleozoic rocks crop out in the western part of the island, also called "Crystalline Corsica" whereas its eastern part, or Alpine Corsica, consists of Mesozoic ophiolites and sedimentary rocks thrust to the West during the Cenozoic Alpine orogeny (Fig. 1; Durand-Delga and Rossi 1991). Paleozoic rocks are also involved in the Alpine nappes but

the intense Cenozoic structural and metamorphic overprints preclude any analysis of the Variscan relics. Most of the Paleozoic formations consist of Permian and Carboniferous volcanic and plutonic rocks (Vellutini 1977; Orsini 1980; Rossi and Cocherie 1991; Cocherie et al. 2005a; Rossi et al. 2005, 2006, 2009). The country rocks of the huge Corsica batholith consist of numerous but relatively small-sized (1 to 20 km) patches widespread throughout Western Corsica (Fig. 1, Ménot and Orsini 1990; Durand Delga and Rossi 1991; Lardeaux et al. 1994). From South to North, they are exposed in the Porto Vecchio, Fautea, Solenzara, Zicavo, Vignola, Topiti, Argentella, Belgodere, S^{ta}-Lucia-di–Mercurio, and Tenda-Agriates-"brown rocks" areas. Among these septa, two groups are distinguished, namely: i) Variscan metamorphic units, and ii) Neoproterozoic metamorphic rocks overlain by Paleozoic sedimentary formations (Durand Delga and Rossi 1991; Rossi et al. 1995, 2009). In the following, the main lithological, structural, and metamorphic features of the largest septa will be presented. Then a general interpretation of the Corsica-Sardinia segment will be discussed at the scale of the Variscan belt.

Pre-Variscan Neoproterozoic septa and their Paleozoic cover

Argentella septum

This area, located to the N of Porto (Fig 1), is surrounded by Late Carboniferous-Permian magmatic rocks to the West and South, and by Lower Carboniferous (Visean) Mg-K granitic intrusions to the North and East. The Argentella septum consists of a Neoproterozoic metamorphic unit unconformably covered by Paleozoic sedimentary rocks (Krylatov and Mamet 1960; Baudelot et al. 1981; Vellutini et al. 1985; Gonord et al. 1992; Rossi et al. 1995, Fig. 2). The metamorphic rocks are micaschists, metagrauwackes, quartzites and amphibolites. The metabasite yields a poorly defined Sm/Nd isochron at 747±100 Ma (Rossi

et al. 1995). The flat-lying foliation developed under greenschist facies metamorphic conditions contains intrafolial folds. It is also deformed by NNW-SSE striking upright folds. The terrigenous sedimentary suite that unconformably overlies the Neoproterozoic metamorphic rocks contains a conglomerate with cm-sized quartz pebbles yielding Early Ordovician zircons dated at 476±26 Ma (Rossi et al. 1995, Fig. 2). The upper part of this series consists of black shale, quartzite, and black chert with Llandoverian graptolites (Barca et al. 1996). Furthermore, to the South of this area, a Late Devonian-Early Carboniferous turbiditic "Culm" series with a Famennian-Strunian limestone layer crops out. In spite of lack of detailed stratigraphic constraints, the Ordovician unconformity argues for the existence of a Neoproterozoic metamorphic basement.

Agriates-Tenda "brown rocks"

Due to the Alpine overprint and weathering, the "brown rocks" (Termier and Maury 1928) crop out along a submeridian trend from the Agriates area in the western Tenda massif up to Corte (Fig. 1). These rocks are hornfelses due to the Late Paleozoic thermal metamorphism induced by the granitic plutons. Some of these rocks form 1m to 100m-scale lensoidal xenoliths within the plutons. The protoliths of the "brown rocks" are micaschists, metasandstones, and amphibolites similar to those described in the Argentella septum. In the Agriates septum, Neoproterozoic metapelites are unconformably covered by Carboniferous (Westphalian) conglomerate and coarse grained sandstone with quartzite, micaschist, rhyolite, andesite, and granite pebbles supplied by the underlying formations (Fig. 2; Rossi et al. 2001). The youngest granitic pebbles yield zircons dated at ca 322± 8 Ma (Rossi and Cocherie 1991). Lower Permian granites dated at 287±4 Ma intrude the Carboniferous series (Rossi and Cocherie 1991).

Variscan Metamorphic septa

Zicavo septum

Lithological succession

30km East of Ajaccio, this septum is entirely bounded by subvertical faults, and intruded by Carboniferous plutons (Fig. 3). Several well foliated and lineated NE dipping metamorphic rocks crop out along a NNW-SSE trend. From bottom to top, three main litho-structural successions are recognized (Vezat 1986, 1988; Thevoux-Chabuel et al., 1995). 1) An augen orthogneiss of ca 1000 m thick represents the lowermost unit. K-feldspar augen are good markers of the ductile deformation (Fig. 4). 2) The overlying unit consists of cm- to m-scale alternations of foliated hornblende plagioclase amphibolites, and fine-grained acidic gneiss with quartz and plagioclase. Such a rock assemblage, well known in many parts of the Variscan belt, is referred to as "leptynite-amphibolite series". The protoliths were lava flows and volcanic-sedimentary rocks of acidic and basaltic compositions. This bimodal magmatism is generally interpreted as formed in an intracontinental rift setting of Ordovician age (e. g. Pin and Peucat 1986, Santallier et al. 1988). Along the road from U Vergajiu to Zicavo, a ca 5 m large serpentinite lens is included within the leptynite-amphibolite series. According to previous analyses, its protoliths was a metaharzburgite (Vezat 1986). Several m-thick layers of biotite-garnet-staurolite micaschist are intercalated in the leptynite-amphibolite series. Furthermore, though not mentioned by previous works, metaconglomerates lenses are also recognized. Flattened and stretched pebbles of quartzite, microgranite, and rhyolite with sizes ranging from 0.1 to 10 cm are included in a fine grain quartzo-feldspathic matrix (Fig. 4). 3) Metapelites overlies the leptynite-amphibolite series (Fig. 3). On the basis of mineralogical composition, sericite micaschist, biotite-muscovite-garnet ± staurolite micaschist, quartz schist, and chlorite-quartz-sericite-graphite micaschist are described (Vezat 1986). In the

structural map (Fig. 3), only a lower- and upper-parts formed by two mica micaschist, and by black micaschist, respectively are distinguished.

Structural analysis of the Zicavo septum

All these lithologies experienced a ductile deformation characterized by a low angle foliation dipping 30° to 60° to the NE (Fig. 3). Locally, in the orthogneiss, close to the contact with the leptynite-amphibolite series, or near the boundary with the garnet micaschist, mylonitic zones, characterized by mineral grain size reduction, and a pervasive stretching lineation argue for localized intense shearing. Two phases of ductile deformation, namely D1 and D2, with contrasted kinematics and pressure-temperature conditions are recognized.

The augen orthogneiss yield a N40°E striking stretching lineation, L1, represented by the elongation of K-feldspar porphyroclasts, and the development of biotite or quartz pressure shadows around the clasts (Fig. 4). A similar L1 stretching lineation is formed by the preferred orientation of hornblende needles in the amphibolite and by the elongation of quartz and feldspar ribbons in the leptynite. The stretching of the pebbles in the conglomeratic layers complies with the NE-SW strike of L1. More rarely, intrafolial folds with axes parallel to L1 develop in the leptynite-amphibolite or in the conglomeratic series (Fig. 4). Numerous kinematic indicators, such as asymmetric pressure shadows around clasts in metaconglomerate, shear bands in orthogneiss, sigma-type porphyroclast systems in augen gneiss and amphibolite are observed both at the outcrop and microscope scales. All criteria consistently indicate a top-to-the-SW sense of shear (Figs. 4, 5). In the mylonitic zones, clast recrystallization forms polycrystalline ribbons of dynamically recrystallized grains with an oblique shape fabric. Sigmoidal mica also indicates a top-to-the-SW shearing (Fig. 5).

This early deformation, D1, is coeval with the crystallization of biotite, garnet, staurolite, in the micaschist or hornblende and plagioclase in amphibolite. Though previously reported

(Vezat 1986; Thevoux-Chabuel et al. 1995), kyanite has not been observed during this study. Nevertheless, the synkinematic mineral assemblages indicate that the D1 deformation developed under amphibolite facies P-T conditions.

The upper part of the structural pile, the micaschist unit, and partly, the leptynite-amphibolite unit, exhibit another stretching lineation, L2, striking NW-SE (N140°E to N170°E, Fig. 3). In the black micaschist, foliation-parallel quartz veins, sometimes folded or boudinaged, (Fig. 4) develop along low temperature m–scale shear zones. Shear bands indicate a top-to-the-SE kinematics. In thin sections cut perpendicular to the foliation and parallel to the NW-SE L2 lineation, biotite and chlorite pressure shadows indicate a top-to-the-SE sense of shear (Fig. 5). Staurolite clasts, wrapped by the foliation, indicate also a top-to-the-SE shearing. Both garnet and staurolite appear as early grains crystallized during D1, and deformed under brittle conditions during D2. Moreover, some garnet grains contain spiral shaped graphitic-quartz inclusions. However, these inclusions are not in continuity with those of the matrix, but separated by an inclusion-free garnet rim suggesting that these inclusions preserved an early structure. Furthermore, the shape of the spiral inclusions is not in agreement with the top-to-the-SE D2 kinematics inferred by chlorite pressure shadows that crystallized under retrogressive conditions. Thus the helicitic inclusions might have developed before D2, possibly during D1. SE-verging folds with low angle axial planes that comply with the D2 kinematics deform the amphibolite and micaschist D1 foliation.

In conclusion, the Zicavo septum documents the tectonic superposition of three lithological and structural units, from bottom to top, orthogneiss, leptynite-amphibolite, and micaschist units. This architecture is the result of two main ductile and synmetamorphic events. The first one, D1, responsible for the stacking from the NE to the SW of the three units, is coeval with an amphibolite facies metamorphism. The D1 foliation is folded and early garnet and staurolite are sheared by a top-to-the-SE, D2 event, coeval with the

development of garnet-chlorite-sericite assemblage under retrogressive conditions. The D2 event is interpreted to accommodate the exhumation of the early D1 structures.

Porto Vecchio septum

Lithological succession

This septum, exposed along the SE coast (Fig. 1), is the southernmost one of Variscan Corsica, bounded by granitoids to the West, and partly overlain by undeformed Eocene sandstone and conglomerate (Fig. 6). In spite of its limited extension, the Porto Vecchio septum displays lithological and structural similarities with the Zicavo area since from bottom to top, or from the SW to the NE, an augen orthogneiss is overlain by a leptynite-amphibolite series followed by a micaschist-paragneiss unit.

In all lithologies, the foliation strikes NW-SE, and dips to the NE (Fig. 6). The biotite of the augen orthogneiss is partly chloritized. This orthogneiss was dated, by U/Pb method on zircon, at 465+19/-16 Ma (Rossi et al., 2009), which corresponds to the age of the porphyritic granite protoliths. The leptynite-amphibolite series is similar to the bimodal magmatic suite described in the Zicavo septum. The terrigenous unit consists of mm- to 10cm-sized clasts of quartz and feldspar enclosed in a fine grain quartz-feldspar matrix yielding biotite, garnet, sillimanite and muscovite. Kyanite clasts are surrounded by a cordierite-spinel symplectitic corona during its retrogression (Libourel 1985; Giacomini et al. 2008). Furthermore, foliation-concordant or -discordant quartz-feldspar veinlets argue for an incipient melting of this para-derived protoliths (Fig. 7).

Structural analysis

In agreement with a previous work (Giacomini et al. 2008), three deformation events are recognized in this septum. The last one that also involves late granitoids will not be considered here, only the first two events, D1 and D2 are presented below. The foliation pervasively developed in the Porto Vecchio area consistently dips to the NE (50 to 60°), and to the North of the study area; it becomes steeper (80° to 90°), even locally, the foliation is overturned, and dips to the SW (Fig. 6). In the orthogneiss, the K-feldspar augens are elongated in the NE-SW (N50E to N80E) direction. Quartz rods, and mica fibers also define this stretching and mineral lineation L1. The northern border of the orthogneiss massif is often mylonitized with pervasive foliation and lineation. Sigma-type porphyroclast systems, and sigmoidal micas indicate a top-to-the-SW sense of shear. In the amphibolite tight isoclinal folds deform the foliation (Fig. 7). Hornblende grains define the NE-SW striking L1 linear fabric, but kinematic indicators are not observed. In the micaschist-paragneiss unit, L1 has not been recognized, the S1 foliation is cut by subvertical or NE-dipping shear surfaces that contain a E-W to NE-SW striking high temperature slickenline, L2, marked by mica or sillimanite fibers. Shear band asymmetry, indicates a normal-dextral sense of shear, with the northern side moving downward with respect to the southern one (Figs. 7, 8). The L1 and L2 microstructures developed under different P-T kinematics, time, and tectonic setting. L1 is coeval with the amphibolite facies metamorphism associated with the southwestward thrusting of the leptynite-amphibolite series above the orthogneiss during the D1 event, whereas L2 that overprints the S1 foliation is associated with anatexis of the metapelitic series during the D2 exhumation of the underlying litho-tectonic units.

In summary, the Porto Vecchio area rocks experienced the same structural evolution than those of the Zicavo one with an early top-to-the-SW D1 thrusting followed by a late top-to-the-E, or SE, D2 extensional shearing. In contrast with the Zicavo area, the Porto Vecchio

septum exposes rare incipient melted rocks that widely develop to the North in the Solenzara-Fautea septum.

Solenzara-Fautea septum

Lithological succession

In this area, rocks are well exposed along the seashore. Although separated by the Eocene sandstone of the Favone graben, the two septa are grouped together (Fig. 9). Migmatite, enclosing restites of mafic or acidic rocks, and rare marble, is the main rock type (Arthaud and Matte 1977; Libourel 1985; Rouire et al. 1993; Giacomini et al. 2008). Metatexite and diatexite are dominant in the southern and northern part of this septum, respectively. The leucosome, consists of quartz, K-Feldspar, muscovite, and the mesosome contains quartz, K-feldspar, biotite, sillimanite, muscovite. Restites are more developed in the southern part than in the northern one. South of Favone, HP felsic granulites, containing garnet, kyanite, K-feldspar, plagioclase, rutile, are well exposed along the coast (Figs. 7, 9). These rocks are generally highly retrogressed, as shown by cataclastic kyanite surrounded by skeletal garnet rimmed by biotite, often crystallized as asymmetric pressure shadows (Fig. 8). Sometimes, kyanite grains are partly or totally pseudomorphosed into a fine grain white mica aggregate. Mafic rocks, namely eclogites and plagioclase-garnet mafic granulite (pyrigarnites) also occur as restites in the migmatite. These rocks are retrogressed into granulite, and then amphibolite in which clinopyroxene and garnet are replaced by hornblende or biotite, respectively.

Structural analysis

Though an early foliation formed by the preferred orientation of kyanite and K-feldspar can be inferred in the HP rocks, the main regional foliation corresponds to that observed in the metatexite developed under amphibolite facies conditions. This macroscopic S2 foliation

presents highly variable directions at the scale of the entire Solenzara-Fautea septum. A N-S to NE-SW trend with eastward dips (50° to 80°) dominates in the Solenzara septum whereas NE-SW to E-W strikes, with still high dip angles, dominates in the Fautea septum (Fig. 9). A scattered mineral lineation is observed in S2. The foliation is also deformed by NE-SW striking post-folial folds. Globally, the foliation attitude suggests a domal structure mostly disrupted by the Late Carboniferous granitic intrusions. The limited exposures do not allow us to depict the whole structural pattern of the Solenzara-Fautea migmatitic domain. Nevertheless, in this area, the metatexites and diatexites can be considered as the same melting event as the incipient migmatization recognized in the Porto Vecchio area. In both areas, crustal melting superimposes upon an earlier event, structurally well recognized by top-to-the-SW ductile shearing in Porto Vecchio area, and by HP metamorphic conditions in Solenzara-Fautea one.

Belgodère septum

Lithological succession

The Belgodère septum is the largest one in Variscan Corsica (Fig. 1). Its strikes N-S along ca 30km, for a maximum width of ca 7km, intruded by Early (on the W), and Late (on the E) Carboniferous granites, and unconformably covered by undeformed Eocene sandstone. The dominant lithology consists of diatexite and metatexite including cm- to km-sized restites. Medium grained leucogranite considered as granitic melts coeval with the migmatite are exposed near Vallica. In the eastern part of the Belgodère septum, a leptynite-amphibolite series and micaschist form km-sized continuous exposures (Palagi et al. 1985; Rossi et al. 2000; Fig. 10). Another piece of the leptynite-amphibolite series and metagabbro can be observed S of Belgodère. This series, similar to those of Zicavo and Porto Vecchio, consists of alternations of acidic gneiss and amphibolites. The protoliths of the later are volcanic-

sedimentary rocks or mafic lavas. In the less foliated amphibolites, gabbroic magmatic textures all still preserved. Garnet amphibolite crops out sporadically. In these rocks, a plagioclase-amphibole-epidote symplectite surrounding garnet argues for the retrogression of an early high-pressure metamorphic stage, probably corresponding to eclogite facies conditions (Palagi et al. 1985). East of Vallica, km-scale restites of augen orthogneiss, and biotite-muscovite-garnet±staurolite micaschist are well exposed. Along the Asco valley, and west of Vallica, paragneiss of volcanic-sedimentary origin, and metaconglomerate with 0.1 to 10 cm sized quartz or feldspar clasts form 1 to 5m large restitic layers. The rarity of preserved protoliths does not allow a precise reconstruction of the pre-migmatitic regional architecture of the Belgodère septum. On the basis of our lithological and structural observations around Belgodère, Vallica, and Asco, the high grade rocks, mainly amphibolites, and leptynite-amphibolite series crop out in the western and eastern parts of the septum, whereas its core is dominated by metapelites and metaconglomerates.

Structural analysis

The migmatitic foliation consistently dips to westward at variable angles (Fig. 10). To the West, the average dip angle is lower than it is to the East, and thus the foliation defines a km-scale antiform overturned to the East (Fig. 11). Cm- to m-scale east-verging folds with N-S to NNE-SSW striking axes comply with the km-scale antiform with its overturned eastern flank (Figs. 11,12). Within the migmatite, syn- and post-anatectic kinematic indicators are rare, but sigmoidal restite and sheared leucosomes also comply with a top-to-the-E shearing (Fig.12). Mineral lineations, represented by hornblende needles, are recognized in the leptynite-amphibolite series, but the subsequent annealing erased the associated kinematic indicators. An E-W striking stretching lineation is defined by the elongated clasts in the metaconglomerate, and by the boudinage of amphibolite layers (Fig. 11). In thin section of

amphibolite, paragneiss, conglomerate, and micaschist cut parallel to the lineation and perpendicular to the foliation, kinematic indicators such as sigmoidal clasts, asymmetric pressure shadows, mica fish, and shear bands indicate a top-to-the-E sense of shear (Fig. 13).

In summary, the Belgodère septum experienced a polyphase structural and metamorphic evolution with an early high pressure event with unknown kinematics, followed by a MP/MT (amphibolite facies) retrogression coeval with E-directed shearing. Lastly, a thermal event is responsible for a widespread crustal melting exposed in the core of an east-vergent asymmetric antiform. The mechanisms responsible for this structure, such as diapir or E-W shortening, have not been investigated here. Although the lithology is quite similar to those described in the Zicavo, Porto Vecchio, and Solenzara-Fautea septa, the Belgodère septum appears as original since structural analysis documents an east-directed shearing, at variance to the SW-directed kinematics in the previous ones. The significance of this feature will be discussed in the following sections.

Topiti septum

This septum, cropping out along the seashore North of Ajaccio (Fig. 1), is the smallest one of this study. Its interest lies in the occurrence of serpentinized harburgite, amphibolites, and amphibole gneiss (Ferré 1989; Tommasini, 1993). In the field, the subvertical foliation strikes NE-SW to NW-SE due to folds with high angle dipping vertical axes. A mineral and stretching lineation formed by the preferred orientation of amphibole needles, and quartz feldspar aggregates dips at a high angle (Fig. 12). Kinematic indicators are rare, but a few asymmetric quartz or amphibole aggregates fabrics indicate a top-to-the-SW shearing.

Vignola septum

West of Ajaccio, migmatite crops out as km-scale xenoliths within Late Carboniferous granitoids (Fig1). The dominant lithology is a quartz-plagioclase-biotite metatexite derived from a paragneiss protolith. Mafic biotite-hornblende restites within the migmatite crop out locally. The N-dipping foliation is well developed but mineral lineation is absent. This small-scale septum has not been studied in detail.

S^{ta}-Lucia di Mercurio complex

Between the SE termination of the Balagne area and N. of Corte, the S^{ta}-Lucia di Mercurio complex (Fig. 1) consists of plutonic rocks: gabbro, norite, diorite, granodiorite, and HT acidic granulites covered by Mesozoic sedimentary rocks (Durand Delga and Rossi 1991; Rossi et al. 1994). According to Libourel (1985), these HT granulites that do not exhibit any Neoproterozoic (Cadomian), nor early Variscan structure or metamorphism were formed during the late Variscan thermal re-equilibration of the Variscan crust. This lithological assemblage presents strong similarities with the lower continental crust exposed in the Ivrea zone of the Alps. Its present exposure is due to W-directed Alpine thrusting. Due to its limited bearings on the early Variscan evolution of Corsica, in the following, the S^{ta}-Lucia di Mercurio complex will not be considered.

Geochronological constraints

Available ages

Several radiometric data are already available for most of the Variscan septa described above. The main results (Fig. 14) are synthesized in Rossi et al. (2009), recent ages for the

migmatites are provided in Li et al. (2012; in review), and new monazite chemical U-Th-Pb data are presented in the next section.

The Zicavo and Porto Vecchio orthogneiss yield U-Pb zircon at 458±32 Ma and 465+19/-16 Ma Ma, respectively. In spite of their large uncertainty, these ages are interpreted as those of the granitic magmatic protoliths. In Belgodère, zircons from a fine grain orthogneiss provided an U-Pb zircon SHRIMP age of 476±8 Ma, Rossi et al., 2009). All these data are close to the ages of similar augen gneiss widespread throughout the entire Variscan Belt, for instance in the Massif Central and Massif Armoricain (e.g. Pin and Peucat 1986; Roger et al. 2004; Cocherie et al. 2005b; Faure et al. 2010 and enclosed references), or in Sardinia where the Lodè orthogneiss was dated at 456±14 Ma (Helbing and Tiepolo 2005). The HP rock (pyrigarnite) of the Solenzara-Fautea septum yields zircon core U-Pb ages at 484±7 Ma, and 440±6 Ma, also interpreted as protoliths age (Rossi et al. 2009). In the same rock, zircon rims are dated at 418±6 Ma and 407±6 Ma (Rossi et al. 2009). These ages are interpreted as close to the age of the HP metamorphism. Moreover, the Solenzara-Fautea granulite yields a zircon U-Pb age at 361±3 Ma, which is considered as that of the granulitic metamorphism (Giacomini et al. 2008). However, they also might represent the age of the metamorphic overprint experienced by the HP rocks during their retrogression from granulite to amphibolite facies conditions.

Zircon U-Pb ages of the migmatite cluster at ca 345-338 whatever the septum, dated mineral, and method (Paquette et al. 2003; Giacomini et al. 2008; Rossi et al. 2009; Li et al. 2012, in review). Recrystallized zircon in the partly migmatized Porto Vecchio paragneiss yields also a 338±4 Ma age (Giacomini et al., 2008). This date, which complies with migmatization, argue for synchronism between the crustal melting and retrogression of the Porto Vecchio paragneiss.

New age constraints

A monazite U-Th-Pb chemical dating of a biotite-garnet micaschist (sample CG 41A, GPS: N 41° 55.118', E 9° 7.064', Fig. 3) from Zicavo has been carried out in order to provide time constraints in this septum (Figs. 3, 15). Macroscopically, this micaschist presents a NNW-SSE striking lineation attributed to the D2 event. In thin section, monazite grains occur in contact with biotite within the rock matrix, suggesting a textural equilibrium with the main metamorphic minerals. In back-scattered electron mode, the dated grains, of ca 50-100 □icrometer size, have an elongated xenomorphic shape without patchy zoning (Fig. 15). The lack of inherited core in the monazite grains argue for a crystallization time coeval with the regional metamorphism. Dating has been performed on 103 analytical spots from 22 grains homogeneously distributed in the thin section. Analytical procedure follows that described in Cocherie et al. (1998) and Bé Mézème et al. (2006). The unimodal age distribution, in agreement with the lack of zonation, suggests that the monazite grains crystallized during a single tectono-metamorphic episode. Therefore, the calculated age at 336 ± 5 Ma can be considered as that of the D2 tectonic-metamorphic extensional event of the Zicavo area. It is worth to note that this age is similar within errors with those of the Porto Vecchio paragneiss (Giacomini et al. 2008; Fig. 13).

Discussion

Correlation between the Corsican Variscan septa

On the basis of the lithological and structural data presented in the previous sections, the Variscan septa can be grouped into two categories. The Topiti, Vignola, Zicavo, Porto Vecchio and Solenzara-Fautea septa are located to the South, or SW, of the Argentella Neoproterozoic basement, whereas the Belgodère septum is located between the Argentella

basement and the Tenda-Agriates “brown rocks”. Within the first group, the Zicavo and Porto Vecchio septa are the most similar, though migmatite is absent in the former. The top-to-the-SW D1 event, also recognized in the Topiti septum, represents the main tectonic-metamorphic phase responsible for crustal thickening, and the top-to-the-SE D2 retrogressive event represents the exhumation phase of the HP rocks, partly coeval with crustal melting. The occurrence of serpentinized harzburgite in Topiti and Zicavo areas, in close proximity with the Neoproterozoic Argentella basement, suggests the existence of a major tectonic boundary between these two contrasted domains. As a working hypothesis, a NW-SE striking boundary, S1, is proposed here (Fig. 16).

Among the Variscan Corsica, the Belgodère septum appears as original, since it exhibits East-directed pre- and syn-migmatitic structures that are not recognized in the other septa. Since these metamorphic rocks developed at the expense of Paleozoic protoliths (e. g. leptynite-amphibolite series, augen orthogneiss), the tectonic and metamorphic evolution of the Belgodère septum must be distinguished from the Argentella Neoproterozoic basement. Its eastern position with respect to the Argentella basement argues for another major boundary, called S2 in Fig. 16, though never exposed in the field. Furthermore, in the Agriates-Tenda area, another Neoproterozoic basement with its Paleozoic sedimentary cover develops eastward of the Belgodère septum.

In summary, although the lack of exposure due to the abundance of Carboniferous granitoids does not allow robust geometric constraints, the available data suggest that Variscan Corsica consists of four tectonic domains, namely from Southwest to Northeast: 1) a Western Domain formed by polyphase Variscan metamorphic rocks, including Topiti, Vignola, Zicavo, Porto Vecchio, and Solenzara-Fautea septa, in which top-to-the-SW D1 shearing, followed by D2 top-to-the-SE shearing and retrogression dominates; 2) the Argentella Neoproterozoic basement and its Paleozoic sedimentary cover undeformed by the

Variscan phases; 3) a northeastern domain represented by the Belgodère septum, characterized by polyphase east-directed structures; 4) the Agriates-Tenda Neoproterozoic basement and its Paleozoic sedimentary cover. The primary arrangement and size of these four Variscan domains, and their S1 and S2 boundaries have been probably modified by Alpine tectonics, however the relative position of one domain with respect to its neighbors might have been globally preserved since large strike-slip faults are not recognized.

Assuming this tectonic subdivision, an interpretative crustal-scale cross-section of the Variscan belt of Corsica is tentatively proposed (Fig. 16). The Western domain represents a stack of metamorphic units thrust to the Southwest (in the present coordinates), and the Belgodère metamorphic unit overthrusts to the east the Agriates-Tenda basement. The S1 and S2 boundaries are interpreted as two suture zones bounding the Argentella Neoproterozoic basement. The main thrust contacts were partly obliterated by crustal melting that gave rise to Early Carboniferous migmatites, followed by the emplacement of the huge Corsican batholith.

The place of Corsica in the East Variscan branch

Taking into account the Tertiary anticlockwise rotation of Corsica-Sardinia (Alvarez 1972; Arthaud and Matte 1977; Edel et al. 1981), Variscan Corsica can be compared with the neighboring massifs of Sardinia and Maures-Tanneron (Fig. 16). It is well acknowledged that the high-grade metamorphic complex of NE Sardinia is similar to the Solenzara-Fautea and Porto-Vecchio ones (e. g. Lardeaux et al. 1994; Franceschelli et al. 2007; Giacomini et al. 2008; Rossi et al. 2009, Cruciani et al. 2013, and enclosed references). In particular, the retrogressed HP eclogites and granulites enclosed as restites in migmatites in NE Sardinia exhibit a similar thermo-barometric evolution than those of the Solenzara-Fautea septa. To the

South (in the present coordinates) of the Posada-Asinara line, the SE-directed thrusts and folds of the Nappe Zone develops with a progressive decrease in metamorphic grade up to the unmetamorphozed External Zone that corresponds to a foreland basin (Carmigani et al. 1994; Elter et al. 1990; Conti et al. 2001; Carozzi and Oggiano 2002). In this scheme, the Corsica Western Domain appears as being the innermost part of the same belt.

The Maures-Tanneron massif is also subdivided into western and eastern parts by the Joyeuse-Grimaud fault correlated with the Posada-Asinara Line (Elter et al. 1990; Bellot, 2005; Corsini and Rolland 2009; Rolland et al. 2009, and enclosed references). According to these works, the Western Maures is comparable with the Nappe Zone of Sardinia. The Eastern Maures is compared to the Sardinia High-Grade metamorphic complex and the Corsica Western Domain as defined above. The similar metamorphic evolution, and the west-directed kinematics documented here comply with this correlation.

Our study allows us to distinguish several tectonic, metamorphic and magmatic events responsible for the present architecture of the Sardinia-Corsica segment. From older to younger ones, the following stages are outlined below. An early high-pressure event, responsible for the eclogite facies metamorphism develops around 420-407 Ma (e.g. Franceschelli et al. 2007; Giacomini et al. 2008). As it is well documented in the Solenzara-Fautea and NE Sardinia, these high-pressure rocks experienced an earlier retrogression with temperature elevation, under granulite facies conditions. The high-pressure metamorphism recorded in the Belgodère metabasites might also be formed at this time. The main top-to-the SW D1 tectonic-metamorphic event, recognized in the Zicavo, Porto Vecchio, and Topiti areas developed under amphibolite facies conditions. The available radiometric constraints argue for a Late Devonian-Early Carboniferous age, at ca 360 Ma, for this event. The D1 event was followed by a top-to-the-SE D2 event, responsible for the exhumation of the metamorphic rocks. In Porto Vecchio and Solenzara areas, the D2 event was coeval with the

crustal melting responsible for migmatization. This event developed during the Visean (345-330 Ma). Lastly, partial melting, probably involving also the lower crust and mantle, gave rise to the emplacement of Mg-K plutonism at ca 340-330 Ma. Variscan migmatization widespread in Corsica involves both the Western and Eastern domains. Thus the geodynamic interpretation of this late- to post-orogenic crustal melting event must consider a general mechanism. It is worth to note that this situation is quite similar to that observed in the Massif Central-Massif Armoricain segment where Carboniferous migmatites are observed in many places (e.g. Faure et al., 2010).

Migmatites intruded by Mg-K plutons are also widespread in the Alpine Variscan basement (Debon and Lemmet 1999; Rubatto et al., 2001), in the Bohemian massif (Holub et al., 1997; Janoušek and Holub, 2007), and in the Vosges massif (Tabaud, 2012). A detail discussion of the origin of this Carboniferous anatexis and plutonism is beyond the scope of this paper but recent hypotheses can be reminded. The origin of Mg-K plutonism might have been the result of: i) involvement of radiogenic-heat production within the subducted continental crust where relaminated radiogenic material would be responsible for both dehydration melting of subducted crust and underlying metasomatized mantle thereby generating the Mg-K magma (Lexa et al., 2011, Tabaud, 2012) or ii) a long-time mantle enrichment above an Early Variscan subduction system followed by melting of this enriched mantle source during the Variscan collision stage due to thermal anomalies possibly created by the sinking of the subducted slab into the mantle (von Raumer et al., 2014). Whatever the right interpretation, the high Mg-K plutonism postdates the development of the main tectonic and metamorphic features, thus it cannot be used as a marker characteristic of a peculiar domain, even if it seems to be restricted to the Southern branch of the Variscan Belt: Vosges, Bohemia, Alpine External Crystalline Massifs, and Corsica.

The Sardinia-Corsica-Maures segment in the Variscan framework

The structural zonation for the Corsica-Sardinia-Maures massif discussed in the previous section points out the similarities of this southeastern Variscan branch with the Bohemian Massif, French Massif Central and Massif Armoricain (e.g. Arthaud and Matte 1977; Franke 2000; Matte 2001; Ballèvre et al. 2009; Faure et al. 2005, 2009a; Schulmann et al. 2009).

The Sardinia foreland basin is similar to the Visean-Namurian turbiditic basin recognized in the S. Massif Central and in the Pyrenees. The low-grade metamorphic rocks of the Outer and Inner Nappe Zone can be correlated with the Fold-and-Thrust Belt and Para-autochthonous Unit of the Massif Central, respectively. The Sardinia High-Grade metamorphic complex and Corsica Western Domain exhibit analogies with the Lower, and Upper Gneiss Units of the Massif Central and Southern Massif Armoricain. In particular, the Zicavo and Porto Vecchio augen orthogneiss are comparable with the Lower Gneiss Unit, and the leptynite-amphibolite series presents striking similarities with those described since a long time in the Massif Central (e.g. Santallier et al. 1988).

In this framework, the Argentella Neoproterozoic basement and its Paleozoic sedimentary cover can be considered as a microcontinent equivalent to Armorica (Rossi et al. 2009). Consequently, the S1 tectonic line would represent the eo-Variscan suture (Fig. 1; Faure et al. 2008). By analogy with the Massif Armoricain, the S2 line that separates the Argentella Neoproterozoic basement and the Eastern Domain (Fig. 16) could be compared with the Conquet-Penzé suture between Armorica and Léon Block, which appears as a small piece of the Mid-German Crystalline Rise in the Saxothuringian Domain (Fig. 1; Faure et al. 2009b). The Corsica-Sardinia-Maures segment presents also some elements of comparison with the Alpine Variscan basement and the Bohemian Massif. The correlation with the Variscan rocks exposed in the Alpine belt remains unsettled yet though several schemes have been hypothesized (e.g. Matte 2001; Guillot and Ménot 2009). The architecture of the

Bohemian massif consists of several litho-tectonic domains, namely from the NW to the SE, they are the Saxothuringian or Mid-German Crystalline Rise (MGCR), Tepla-Barrandian, Moldanubian, and Brunian (or Moravo-Silesian) domains (e.g. Franke 2000; Schulmann et al. 2009 and enclosed references). Both the Saxothuringian and the Tepla-Barrandian domains exhibit a Neoproterozoic basement. The boundary between the Saxothuringian and Tepla-Barrandian domains, characterized by mafic-ultramafic rocks, is considered as an ophiolitic suture resulting of a S-directed subduction. The Tepla-Barrandian Domain contains a well-developed un-metamorphosed Early Paleozoic sedimentary succession. Conversely, in the Moldanubian Domain, the SE-directed synmetamorphic structures are interpreted as the result of the underthrusting of the Brunia continent below the Moldanubian. This framework cannot be directly correlated with that proposed here for the Corsica-Sardinia-segment, nevertheless, similar features appear in both areas such as the bi-vergent structures and the presence of a weakly deformed and un-metamorphosed Early Paleozoic sedimentary sequence. Thus, we tentatively suggest here that if the Tepla-Barrandian Domain is correlated with the Argentella domain, the northern part of the Western Domain, and the Eastern Domain of Corsica might correspond to the Moldanubian, and Saxothuringian-MGCR domains, respectively. Also, one can note that Mg-K plutons emplaced at the same age close to the tectonic contact between homologue domains, either in Bohemia between the Tepla-Barrandian and Moldanubian Domain, or in Corsica between Argentella (i.e. Armorica block) and the high grade Western Domain (Holub et al. 1997). Such a configuration is in agreement with a general reconstruction of the Variscan Belt (Matte 2001; Guillot and Ménot 2009).

Conclusion

In spite of their scattered position within the granitic plutons, the fragments of the Corsican substratum exhibit lithological, structural, and metamorphic features that allow us to suggest a

consistent arrangement at the scale of the island. The possible correlations within the Corsica, Sardinia, and Maures massif show that the bulk architecture of this segment can reasonably be compared with that of the Massif Central, Massif Armoricain, and Bohemian Massif. Nevertheless, in the present state of knowledge, the correlation of the Corsica-Sardinia-Maures segment with the nearest Variscan massifs remains disputable. A comprehensive view of the Corsica-Sardinia-Maures segment with other Variscan massifs of Western Europe requires additional information, particularly on the thermo-barometric evolution, and the timing of the succession tectonic and metamorphic events.

Acknowledgements

Field, and analytical expenses for this study have been supported by the French national program “Carte géologique de la France au 1/50 000 led by BRGM, and a National Natural Science Fundation of China (NNSFC) grant 41273070. Jean-Marc Lardeaux, Guido Gosso, and Karel Schulmann are thanked for their constructive comments to improve the manuscript.

References

Alvarez W (1972) Rotation of the Corsica–Sardinia Microplate. Nature Physical Sscience 235: 103-105

Arthaud F, Matte P (1977) Détermination de la position initiale de la Corse et de la Sardaigne à la fin de l’orogenèse hercynienne grâce aux marqueurs géologiques ante-mésozoïques. Bull Soc Geol France 19: 833-840

Ballèvre M, Bosse V, Ducassou C, Pitra P (2009) Paleozoic history of the Armorican Massif: models for the tectonic evolution of the suture zones. CR Geoscience 341: 174-201

Barca S, Durand-Delga M, Rossi P, Storch P (1996) The Pan-African micaschists of Corsica (France) and their Palaeozoic cover: their place in the Variscan orogen of Southern Europe. CR Acad Sci Paris II 322: 981-989.

Baudelot S, Durand- Delga M, Mirouse P, Perret M-F, Taugourdeau-Lantz J (1981) Le Dévonien de Galeria en Corse septentrionale, sa datation et sa place en Méditerranée occidentale, CR Acad Sci Paris II 292: 347–354.

Bé Mézème E, Cocherie A, Faure M, Legendre O, Rossi P (2006) Electron microprobe monazite geochronology: a tool for evaluating magmatic age domains. Examples from the Variscan French Massif Central. Lithos 87 : 276–288

Bellot J-P (2005) The Palaeozoic evolution of the Maures Massif (France) and its potential correlation with other areas of the Variscan belt: a review. J Virtual Explorer 19 (Paper 4).

Carmignani L, Carosi R, Di Pisa A, Gattiglio M, Musumeci G, Oggiano G, Pertusati P-C (1994). The Hercynian Chain in Sardinia. Geodinamica Acta 7: 31–47

Carosi R, Oggiano G (2002) Transpressional deformation in NW Sardinia (Italy): insights on the tectonic evolution of the Variscan belt. C R Geoscience 334: 287–294.

Cocherie A, Legendre O, Peucat J J, Kouamelan AN, (1998) Geochronology of polygenetic monazites constained by in situ electron microprobe Th–U–total Pb

determination: implications for lead behaviour in monazite. Geochimica Cosmochimica Acta 62, 2475–2497

Cocherie A, Rossi P, Fanning C M, Guerrot C (2005a) Comparative use of TIMS and SHRIMP for U–Pb zircon dating of A-type granites and mafic tholeiitic layered complexes and dykes from the Corsican Batholith (France). Lithos 82: 185– 219

Cocherie A, Baudin T, Autran A, Guerrot C, Fanning M, Laumonier B, (2005b) U–Pb zircon (ID-TIMS and SHRIMP) evidence for the early Ordovician intrusion of metagranites in the late Proterozoic Canaveilles Group of the Pyrenees and the Montagne Noire (France). Bull Soc Géol France 176: 269–282

Conti P (2001) Change of nappe transport direction during the Variscan collisional evolution of central-southern Sardinia (Italy). Tectonophysics 332: 255-273

Corsini M, Rolland Y (2009) Late evolution of the southern European Variscan belt: Exhumation of the lower crust in a context of oblique convergence. C R. Geoscience 341: 214–223.

Cruciani G, Franceschelli M, Massonne H-J, Carosi R, Montomoli C (2013) Pressure-temperature and deformational evolution of high-pressure metapelites from Variscan NE Sardinia, Italy. Lithos 175-176: 272-284

Debon F, Lemmet M (1999) Evolution of Mg/Fe ratios in Late Variscan plutonic rocks from the External Crystalline Massifs of the Alps (France, Italy, Switzerland). J Petrology 40 : 1151-1185.

Durand- Delga M, Rossi P (1991) Les massifs anciens de la France: la Corse. Sci. Géol Mém Strasbourg 44: 311-336

Edel J-B, Montigny R, Tuizat R (1981) Late Paleozoic rotations of Corsica and Sardinia : new évidence from paleomagnetic and K-Ar studies. Tectonophysics 79: 201-203

Elter M, Musumeci G, Pertusati P-C (1990) Late Hercynian shear zones in Sardinia. Tectonophysics 176: 387-102

Faure M, Bé Mézème E, Duguet M, Cartier C, Talbot J-Y (2005) Paleozoic tectonic evolution of Medio-Europa from the example of the French Massif Central and Massif Armoricain. J Virtual Explorer Electronic edition ISSN 1441-8142, 19 paper 5.

Faure M, Bé Mézème E, Cocherie A, Rossi P, Chemenda A, Boutelier D (2008) Devonian geodynamic evolution of the Variscan Belt, insights from the French Massif Central and Massif Armoricain. Tectonics 27: TC2008, http://dx.doi.org/10.1029/2007TC002115

Faure M, Lardeaux JM, Ledru P (2009a) A review of the pre-Permian geology of the French Massif Central. *Comptes Rendus Géosciences*, thematic issue « The Variscan Orogeny » 341: 202-213 doi :10.1016/j.crte.2008.12. 001

Faure M, Sommers C, Melleton J, Cocherie A, Lautout O (2009b) The Léon Domain (French Massif Armoricain): a westward extension of the Mid-German Crystalline Rise? Structural and geochronological insights. International J. Earth Sciences 99: 65-81

Faure M, Cocherie A, Bé-Mézème E, Charles N, Rossi P (2010) Middle Carboniferous crustal melting in the Variscan Belt: New insights from U-Th-Pb_{tot}. monazite and U-Pb zircon ages of the Montagne Noire Axial Zone (southern French Massif Central). Gondwana Research: 633-673

Ferré E (1989) Les gneiss à cordiérite-grenat-orthoamphibole de Topiti (Corse occidentale, France). C R Acad Sci Paris 309: 893-898

Franceschelli M, Puxeddu G, Cruciani G, Utzeri D (2007) Metabasites with eclogites facies relics from Variscides in Sardinia, Italy: a review. Int J Earth Sci 96: 795-815

Franke W (2000) The Mid-European segment of the Variscides: tectonostratigraphic units, terrane boundaries and plate tectonic evolution. Geol Soc London Spec Publ 179: 35-61

Giacomini F, Bomparola R-M, Ghezzo C (2005) Petrology and geochronology of metabasites with eclogites relics from NE Sardinia: constraints for the Paleozoic evolution of Southern Europe. Lithos 82: 221-248

Giacomini F, Dallai L, Carminati E, Tiepolo M, Ghezzo C (2008) Exhumation of a Variscan orogenic complex: insights into the composite granulitic–amphibolitic metamorphic basement of Southeast Corsica (France). J Metamorphic Geol. 26: 403–436

Gonord H, Ménot R-P, Michon G, Pichon H (1992) Le lambeau métamorphique et sédimentaire de l'Argentella (Corse septentrionale) : Indice d'une tectonique tangentielle et implications régionales, Schweiz Mineral Petrol Mill 72: 335-345

Guillot S, Ménot RP (2009) Paleozoic evolution of the External Crystalline Massifs of the Western Alps. C. R. Geoscience 341 : 253–265

Helbing H, Tiepolo M (2005) Age determination of Ordovician magmatism in NE Sardinia and its bearing on Variscan basement evolution. J Geol Soc Lond 162: 689–700.

Holub F V, Cocherie A, Rossi, Ph (1997) Radiometric dating of granitic rocks from the Central Bohemian plutonic complex /Czech Republic): constraints on the chronology of thermal and tectonic events along the Moldanubian-Barrandian boundary. C. R. Acad. Sci., 325: 19-26.

Janoušek V, Holub F V (2007) The causal link between HP–HT metamorphism and ultrapotassic magmatism in collisional orogens: case study from the Moldanubian Zone of the Bohemian Massif. Proc. Geologists' Association 118: 75-86.

Krylatov V-S, Mamet B (1966) Données nouvelles sur les terrains paléozoïques de l'Argentella-Tour Margine (Corse). Attribution à la limite dévono-carbonifère du calcaire de Capitello, Bull Soc Geol France 7: 73-7

Lardeaux J-M, Menot R-P, Orsini J-B, Rossi P, Naud G, Libourel G (1994) Corsica and Sardinia in the Variscan chain. In: Keppie J-D, (ed) Pre-Mesozoic Geology in France and Related Areas. Springer Verlag 468-479

Lexa O, Schulmann K, Janoušek V, Štípská P, Guy A, Racek M (2011) Heat sources and trigger mechanisms of exhumation of HP granulites in Variscan orogenic root. Journal of Metamorphic Geology 29: 79–102.

Li X, Lin W, Faure M (2012) SIMS U/Pb Zircon dating of migmatite and high Mg-K intrusion from the Variscan orogenic complex of Corsica : from crustal anatexis to mantle melting. Géologie de la France 1: 136

Libourel G (1985) Le complexe de Santa-Lucia-di-Mercurio (Corse). Ultramafites mantelliques, intrusion basique stratifiée, paragneiss granulitiques. Un équivalent possible des complexes de la zone d'Ivrée, Ph D thesis Université Paul-Sabatier Toulouse 461 pp

Martínez Catalán J-R, Arenas R, Abati J, Sánchez Martínez S, Días García F, Fernández Suárez J, González Cuadra P, Castiñeiras P, Gómez Barreiro J, Díez Montes A, González Clavijo E, Rubio Pascual F-J, Andonaegui P, Jeffries E, Alcock J, Díez Fernández R, López Carmona A (2009) A rootless suture and the loss of the roots of a mountain chain: the Variscan belt of NW Iberia. CR Geoscience 341: 114-126.

Matte P (1986) Tectonic and plate tectonic model for the Variscan belt of Europe. Tectonophysics 126: 329-374

Matte P. (2001) The Variscan collage and orogeny (480–290 Ma) and the tectonic definition of the Armorica microplate. Terra Nova 13: 122–128

Ménot R-P, Orsini J-B (1990) Evolution du socle anté-stéphanien de Corse: événements magmatiques et métamorphiques. Schweiz Mineral Petrogr Mitt 70: 35–53

Orsini J-B (1980) Le batholite corso-sarde : un exemple de batholite hercynien (structure, composition, organisation d'ensemble). Sa place dans la Chaîne varisque de l'Europe moyenne. Thèse Doct Sci Univ Aix-Marseille III 370 p.

Palagi P, Laport D, Lardeaux J-M, Menot R-P, Orsini J-B (1985) Identification d'un complexe leptyno–amphibolique au sein des « gneiss de Belgodère » (Corse occidentale). C R Acad Sci Paris Ser II 301: 1047–1052

Paquette J-L, Menot R-P, Pin C, Orsini J-B (2003) Episodic and short-lived granitic pulses in a post-collisional setting: evidence from precise U–Pb zircon dating through a crustal cross section in Corsica. Chem Geol 198: 1–20

Pin C, Peucat J-J (1986) Ages des épisodes de métamorphisme paléozoïques dans le Massif central et le Massif armoricain. Bull Soc Géol France 8: 461–469.

Roger F, Respaut J-P, Brunel M, Matte P, Paquette J-L. (2004) Première datation U–Pb des orthogneiss oeillés de la zone axiale de la Montagne Noire (sud du Massif Central): nouveaux témoins du magmatisme ordovicien dans la chaîne Varisque. C R Géoscience 336: 19–28

Rolland Y, Corsini M (2009) Metamorphic and structural evolution of the Maures-Tanneron massif (SE Variscan chain): evidence of doming along the transpressional margin, Bull Soc Geol France 180: 217-230

Rossi P, Cocherie A (1991) Genesis of a Variscan batholith: field, mineralogical and geochemical evidence from the Corsica–Sardinia batholith Tectonophysics 195: 319–346

Rossi P, Durand-Delga M, Caron JM, Guieu G, Conchon O, Libourel G, Loye-Pilot MD (1994) Carte géologique de la France au 1/50000. Carte et Notice explicative de la feuille Corte 150pp BRGM, Orléans, France

Rossi P, Durand-Delga M, Cocherie A (1995) Identification en Corse d'un socle panafricain (cadomien), conséquences sur la paléogéographie de l'orogène varisque sud-européen. C R Acad Sci Paris 321 II: 983-999

Rossi P, Durand-Delga M, Lahondère J-C, Lahondère D (2001) Carte géologique de la France au 1/50000. Carte et Notice explicative de la feuille Santo-Pietro-di-Tenda 224pp BRGM, Orléans, France

Rossi P, Cocherie A, Fanning M, Guerrot C (2005) Comparative use of TIMS and SHRIMP for U-Pb zircon dating of A-type granites and mafic tholeiitic layered complexes and dykes from the Corsican batholith (France). Lithos 82: 185-219

Rossi P, Cocherie A, Fanning M, Deloule E (2006) Variscan to eo-Alpine events recorded in European lower-crust zircon sampled from the French Massif Central and Corsica. Lithos 87: 235-260

Rossi P, Oggiano G, Cocherie A (2009) A restored section of the ‘‘southern Variscan realm’’ across the Corsica–Sardinia microcontinent C. R. Geoscience 341: 224–238

Rossi P, Marre J, Cocherie A, Caballero Y (2010) Carte géologique de la France (1/50 000), carte et notice explicative Vico-Cargese. Orléans BRGM, 156 p

Rouire J, Bourges F, Rossi P, Libourel G (1993) Carte géol. France (1/50 000), Carte et Notice explicative de la feuille Porto-Vecchio. Orléans BRGM 61 p.

Rubatto D, Schaltegger U, Lombardo B, Compagnoni R (2001) Complex Paleozoic magmatic and metamorphic evolution in the Argentera Massif (Western Alps) resolved with U–Pb dating. Schweiz Mineralogische und Petrographische Mitteilungen 81: 213–228.

Santallier D, Briand B, Menot R-P, Piboule M (1988) Les complexes leptyno-amphiboliques (CLA): revue critique et suggestion pour un meilleur emploi de ce terme. Bull Soc Géol France 1: 3-12

Schulmann K, Konopásek J, Janousek V, Lexa O, Lardeaux J-M, Edel J-B, Stipská P, Ulrich S (2009) An Andean type Palaeozoic convergence in the Bohemian Massif. CR Geoscience 341: 266-286.

Tabaud AS (2012) Le magmatisme des Vosges: conséquence des subductions paléozoïques (datation, pétrologie, géochimie, ASM). Thèse Doct Univ Strasbourg 223 p

Termier P, Maury E, (1928) Nouvelles observations géologiques dans la Corse orientale. Essai de synthèse tectonique. C R Acad Sci Paris 186: 1393-1396

Thevoux-Chabuel H, Menot R-P, Lardeaux J-M, Monnier O (1995) Evolution polyphasée dans le socle de Zicavo (Corse-du-Sud): témoin d'un amincissement post-orogénique. C R Acad Sci Paris 321 II: 47-56

Tommasini S (1993) Petrologia del magmatismo calcalcalino del Batolite Sardo-Corso: processi genetici ed evolutivi dei magmi in aree di collisione continentale e implicazioni geodinamiche. Ph.D. Thesis, University of Perugia, 326 pp.

Vellutini P J (1977) Le magmatisme permien de la Corse du Nord-Ouest ; son extension en Méditerranée occidentale. Thèse Doct Sci Univ Aix-Marseille III, 317 p.

Vellutini P J, Orsini JB, Michon G, Brisset F, Cochemé JJ (1985) Carte géologique de la France au 1/50000, feuille Galeria-Osani. Orléans: BRGM. Notice explicative 109pp

Vezat R (1986) Le batholite calco-alcalin de la Corse: les formations calédono-varisques de Zicavo. Mise en place du batholite. Thèse 3ème cycle Univ Toulouse, 370 p.

Vezat R (1988) Meaning of the metamorphic formation of the Zicavo area in the Mediterranean Variscan frame, Southern Corsica C R Acad Sci Paris 306 II: 725-729

von Raumer J-F, Finger F, Veselá P, Stampfli G-M (2014) Durbachites-Vaugnerites, a geodynamic marker in the central European Variscan orogen. Terra Nova 26 : 85–95.

Figure Captions

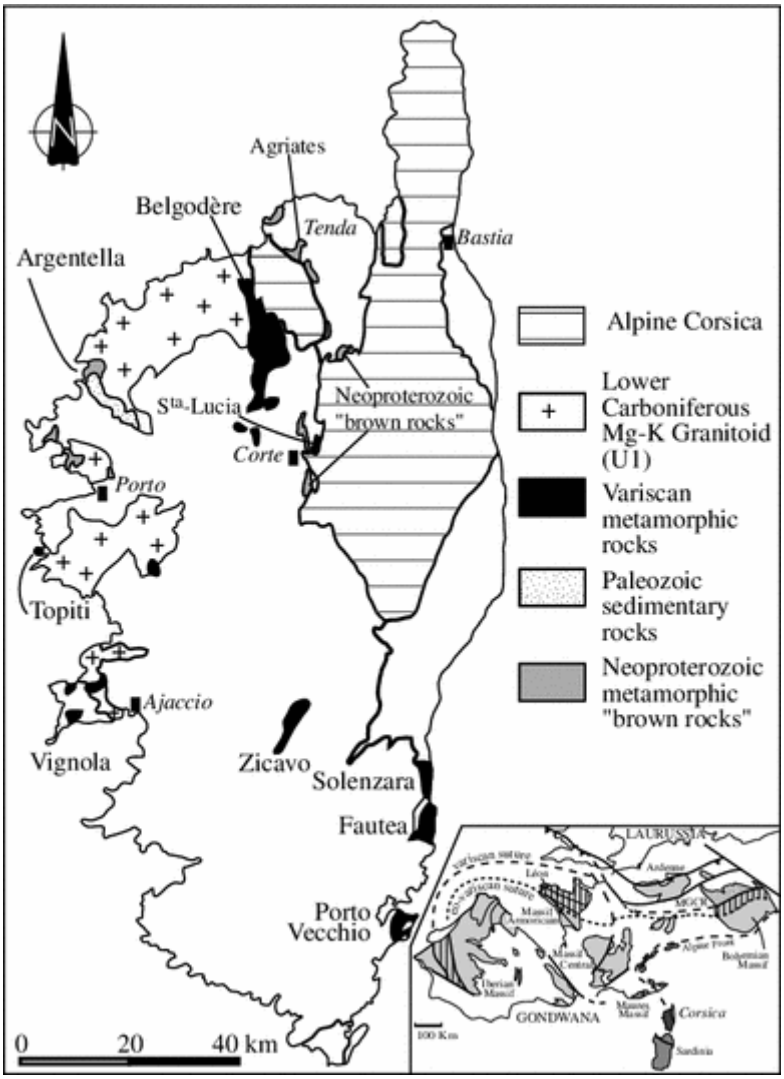

Fig. 1. Structural map of Corsica (simplified from Rossi et al., 1995) showing the Variscan and pre-Variscan septa. Inset : location of the Corsica-Sardinia islands within the Variscan framework. Striped domain: Armorica microcontinent, dotted domain: Léon and Mid-German Crystalline Rise (MGCR).

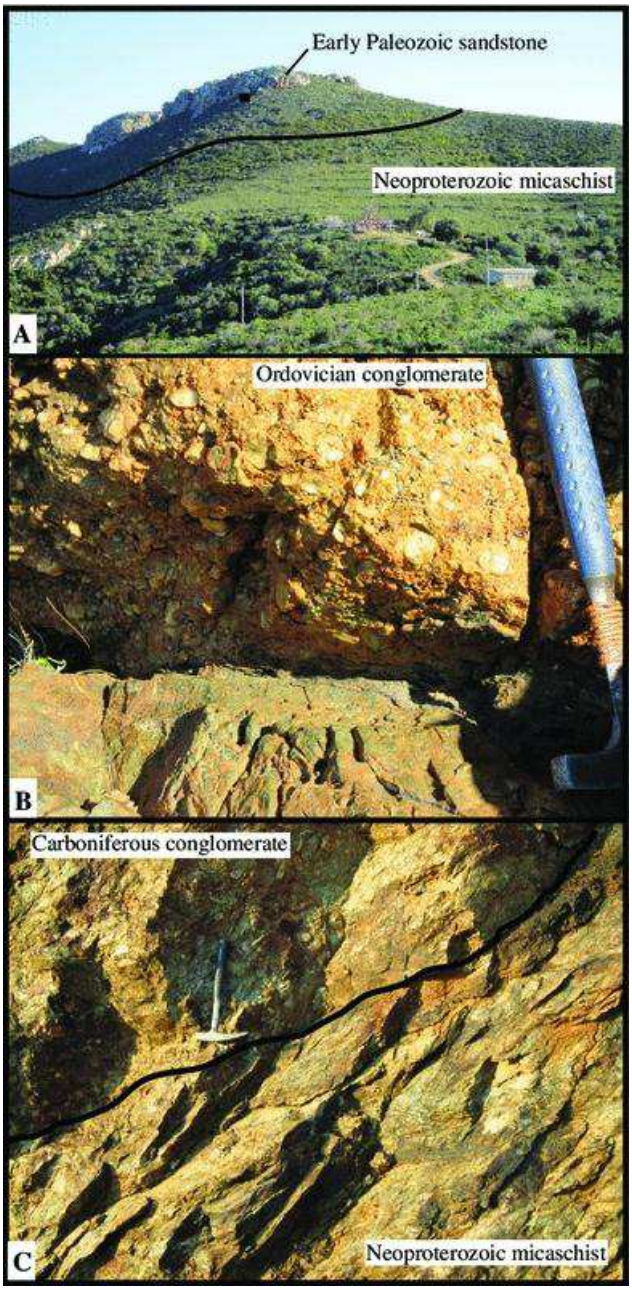

Fig. 2. Field pictures of the Pre-Variscan Neoproterozoic basement. A: Argentella area (black rectangle corresponds to picture B); B: sedimentary contact between upper Ordovician conglomerate and sandstone; C: Carboniferous (Westphalian conglomerate unconformably covering Neoproterozoic micaschist (W. Tenda).

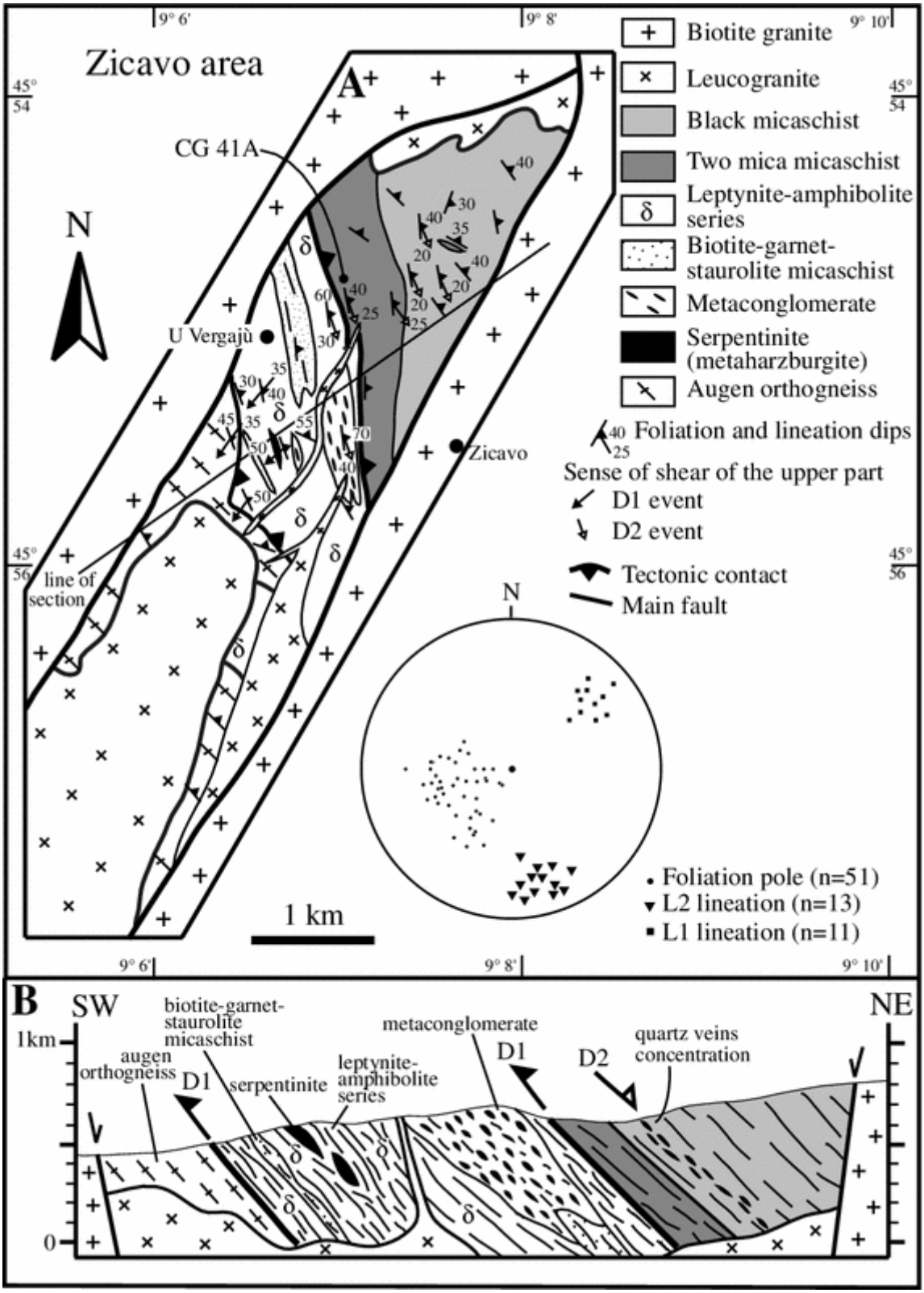

Fig. 3. Structural map, cross section, and stereographic plot of the structural elements of the Zicavo area, (located in Fig. 1), showing the D1 stack of nappes, and D2 exhumation tectonic-metamorphic events.

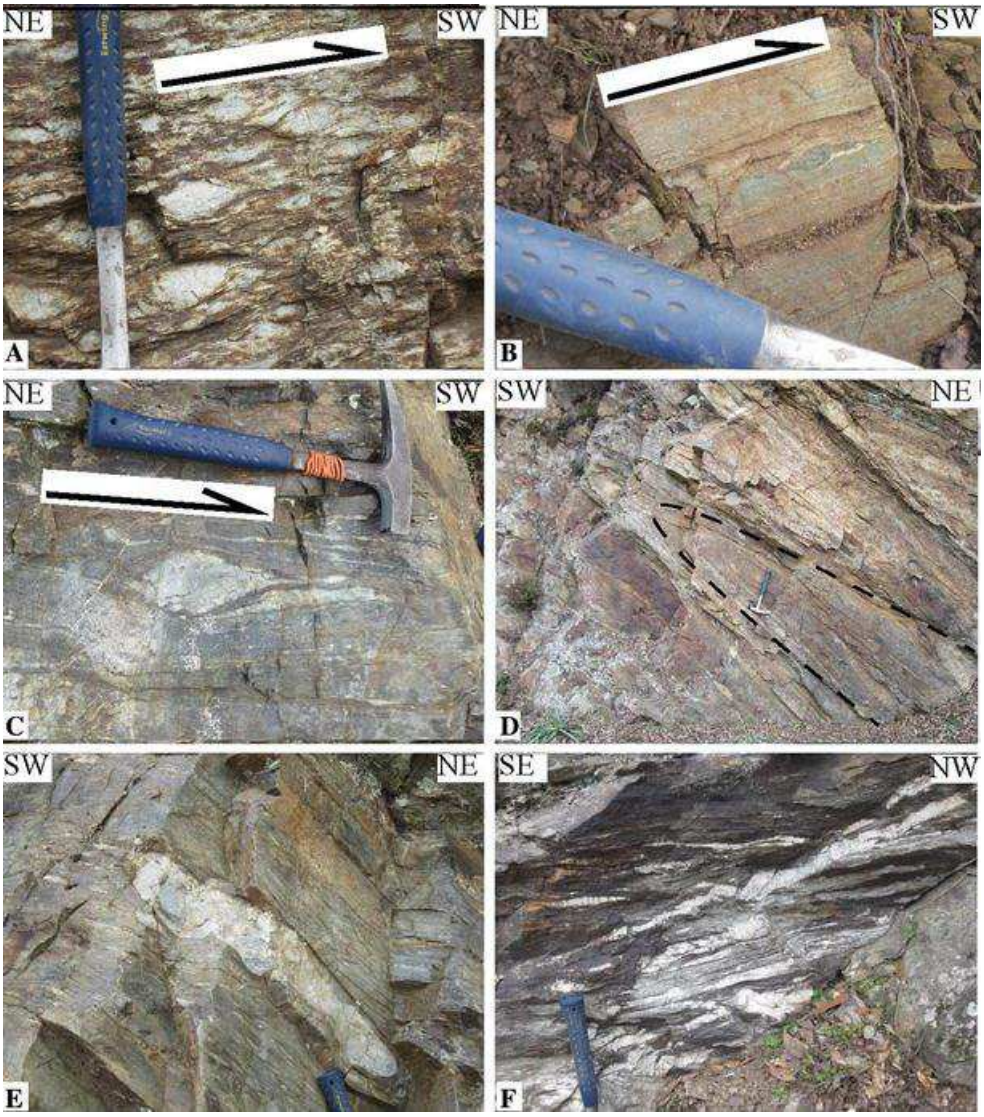

Fig. 4. Field pictures from the Zicavo area. A: Augen orthogneiss with top-to-the-SW D1 kinematic indicators. B: Top-to-the SW D1 sigmoidal amphibole in the leptynite-amphibolite series. C: sigmoidal pebble with top-to-the-SW D1 sense of shear in the metaconglomerate. D: isoclinal fold in quartz metapelite around the metaconglomerate. E: m-scale pebble in the metaconglomerate. F: quartz vein concentration along D2 shear zone in the black micaschist.

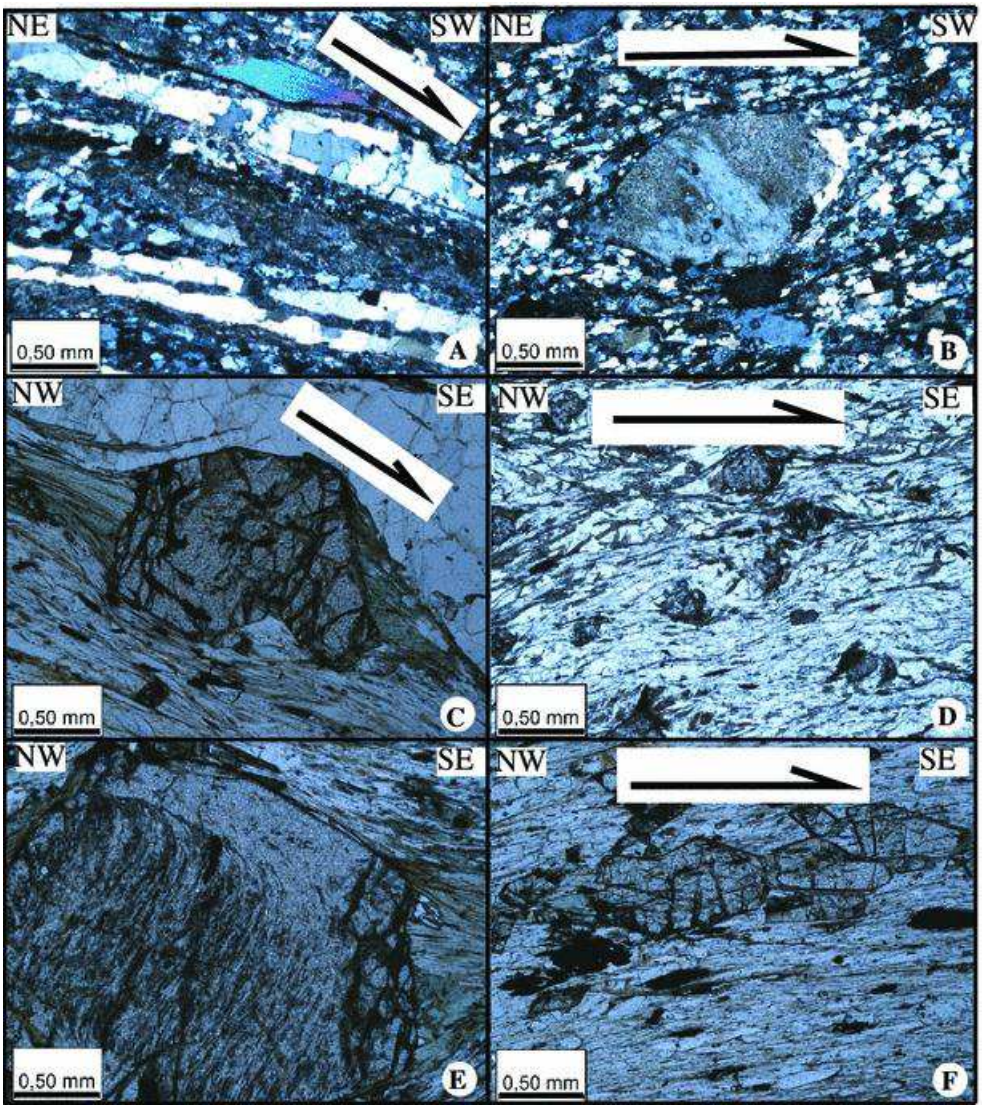

Fig. 5. Microscope-scale D1 and D2 deformation structures of the Zicavo area.

A: Quartzite in the leptynite amphibolite series with top-to-the-SW D1 mica fish and platten quartz; B: quartz grain in metaconglomerate with top-to-the-SW D1 sense of shear; C: garnet surrounded by chlorite pressure shadow indicating top-to-the-SE D2 shearing in two-mica schist; D: D2 biotite pressure shadows around garnet and shear bands in two mica schist; E: detail of D1 helicitic inclusion in garnet core rimmed by inclusion free D2 garnet surrounded by chlorite pressure shadow in two mica schist; E: cataclastic D1 staurolite cracked durint D2 event.

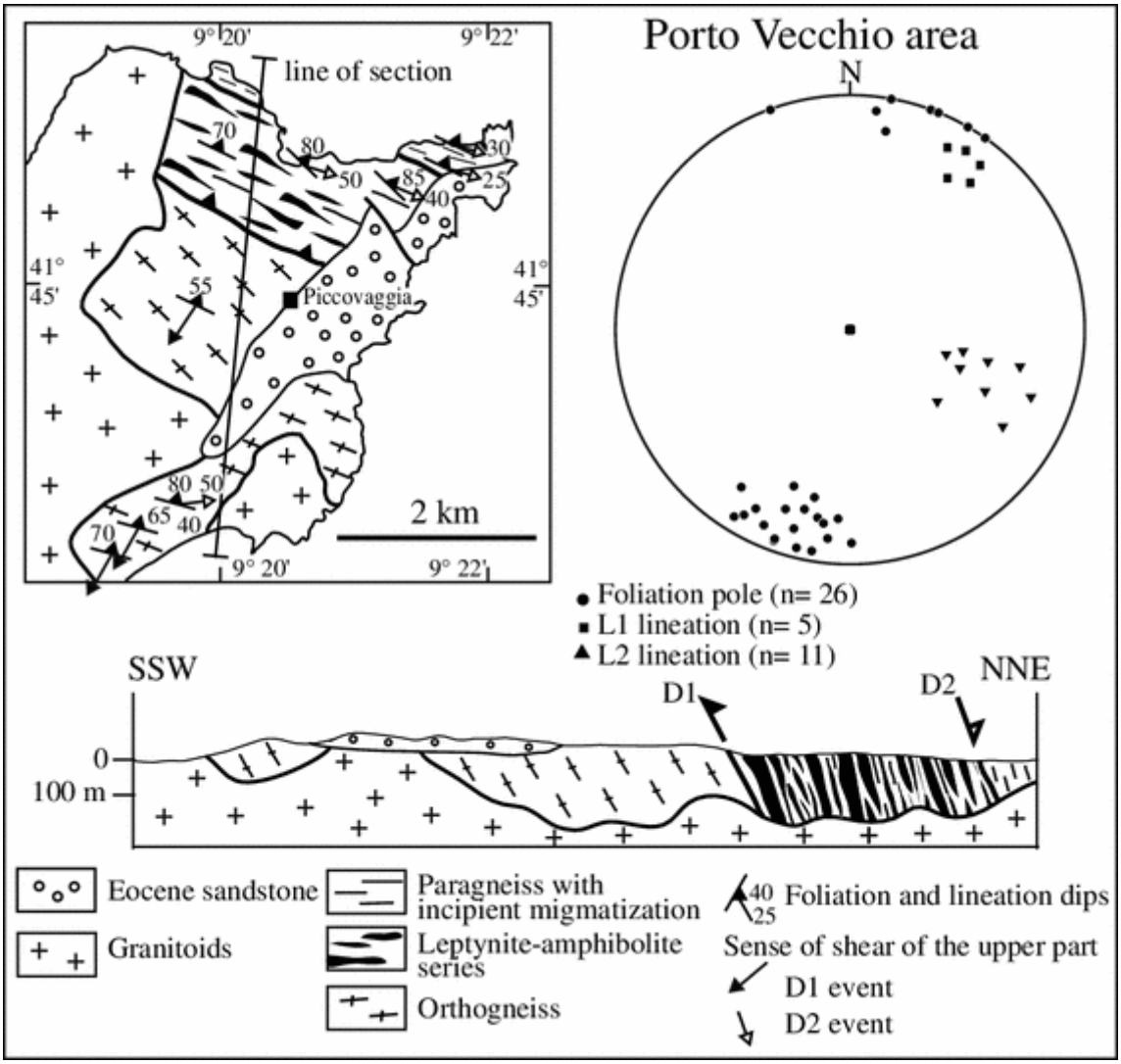

Fig. 6. Structural map, cross section, and sterographic plot of the Porto Vecchio area (located in Fig. 1) showing the top-to-the- NW D1 thrusting of the leptynite-amphibolite series upon the orthogneiss, and the top-to-the-SE D2 extensional shearing.

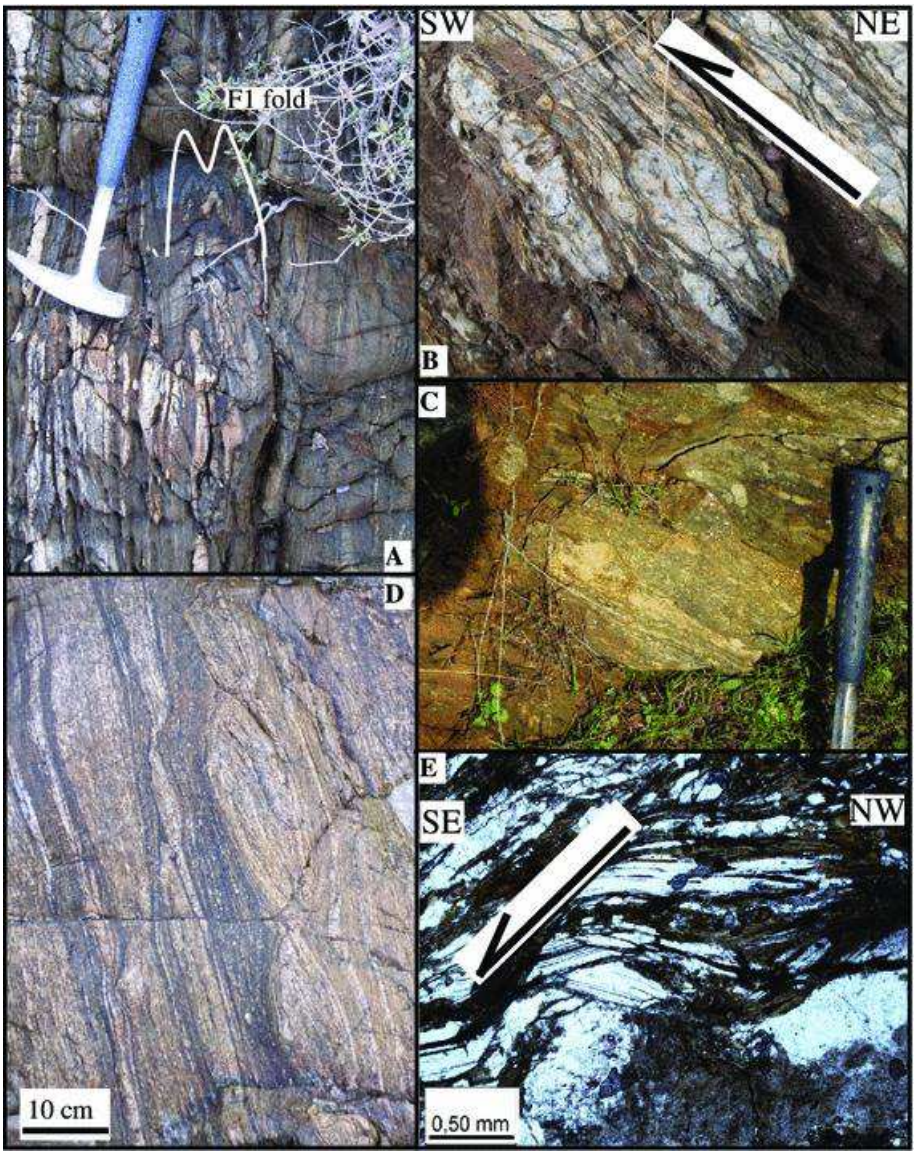

Fig. 7. Field and microscope-scale pictures from the Porto Vecchio (A, B, C, E), and Solenzara-Fautea (D) areas. A: isoclinal fold in the leptynite-amphibolite series; B: Augen orthogneiss with top-to the SW D1 kinematic indicators; C: Biotite-garnet paragneiss with incipient migmatization; D: Paragneiss with HP granulitic metamorphism near Fautea; E: Top-to-the-SE D2 shear band cutting the D1 foliation, (natural light).

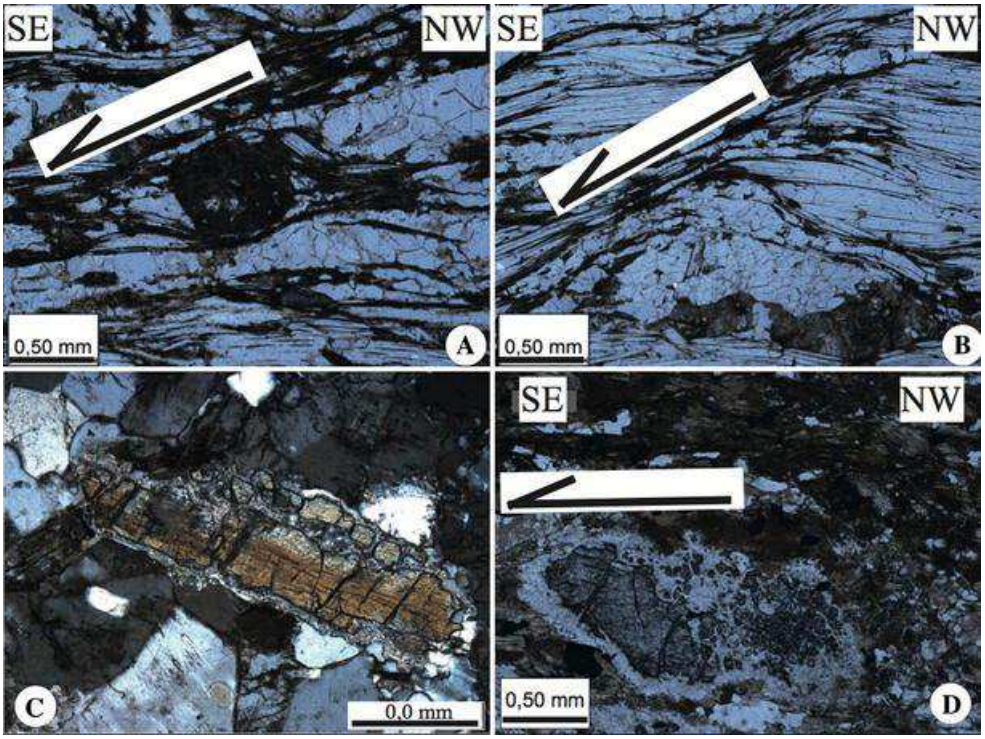

Fig. 8. Microscope-scale deformation structures of the Porto Vecchio (A, B) and Solenzara-Fautea (C, D) areas. A: Asymmetric chlorite pressure shadows indicating top-to-the-SE shearing developed during the D2 event (natural light); B Top-to-the-SE D2 shear band cutting the D1 foliation, (natural light).

C: Thin section of granulitic paragneiss with kyanite relic grain surrounded by retromorphic white mica aggregate, (natural light); D: Catalastic kyanite surrounded by an asymmetric white mica retromorphic aggregate indicating top-to-the-SE shearing, (natural light).

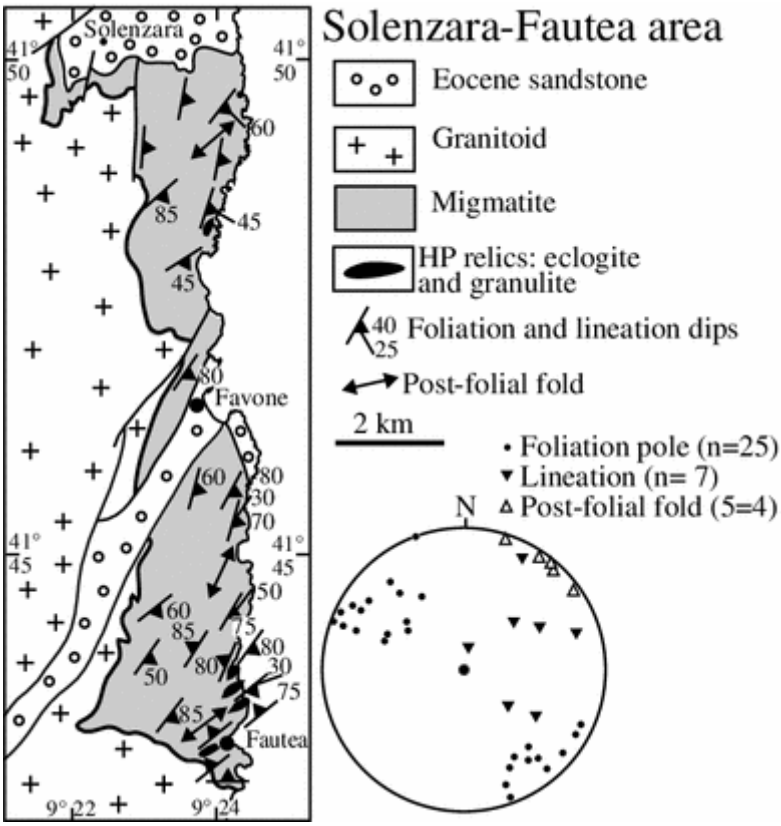

Fig. 9. Structural map, cross section, and stereographic plot of the Solenzara-Fautea area (located in Fig. 1).

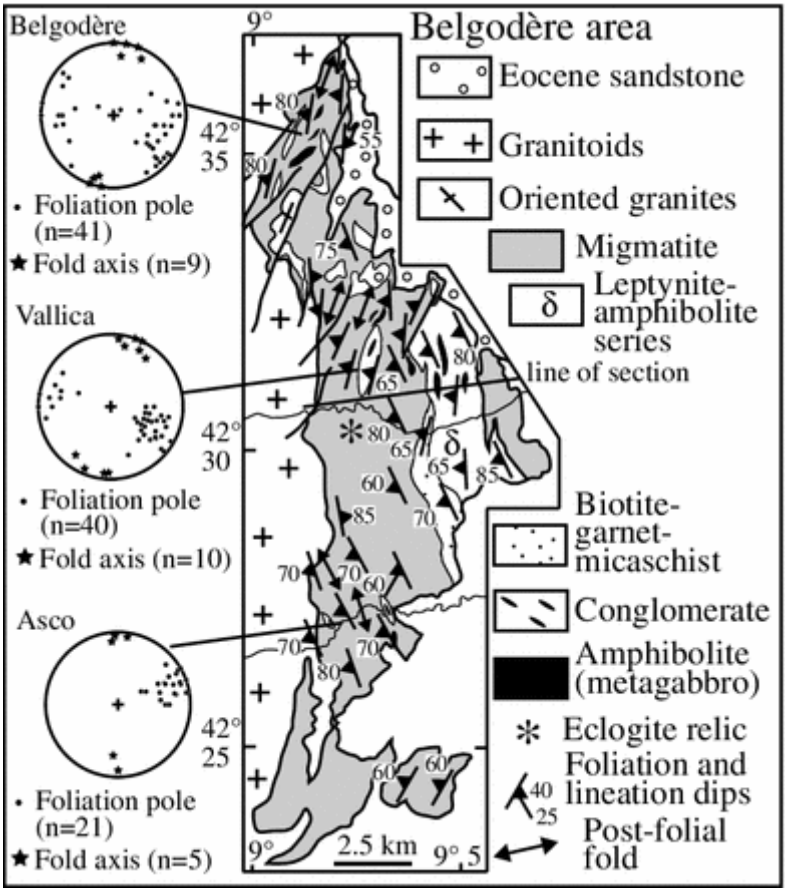

Fig. 10. Structural map, and stereographic plots for the Belgodère, Vallica, Asco, of the Belgodère area (located in Fig. 1).

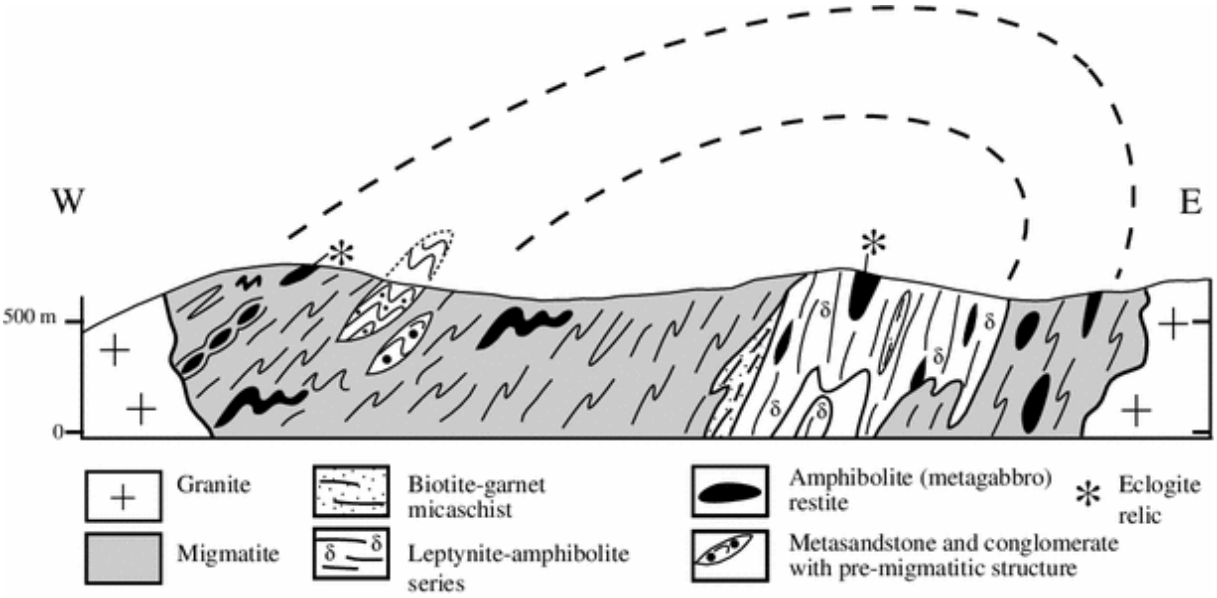

Fig. 11. Cross section of the Belgodère East-verging migmatitic antiform. The restitic rocks (amphibolite, sandstone, conglomerate) are foliated and folded before migmatization.

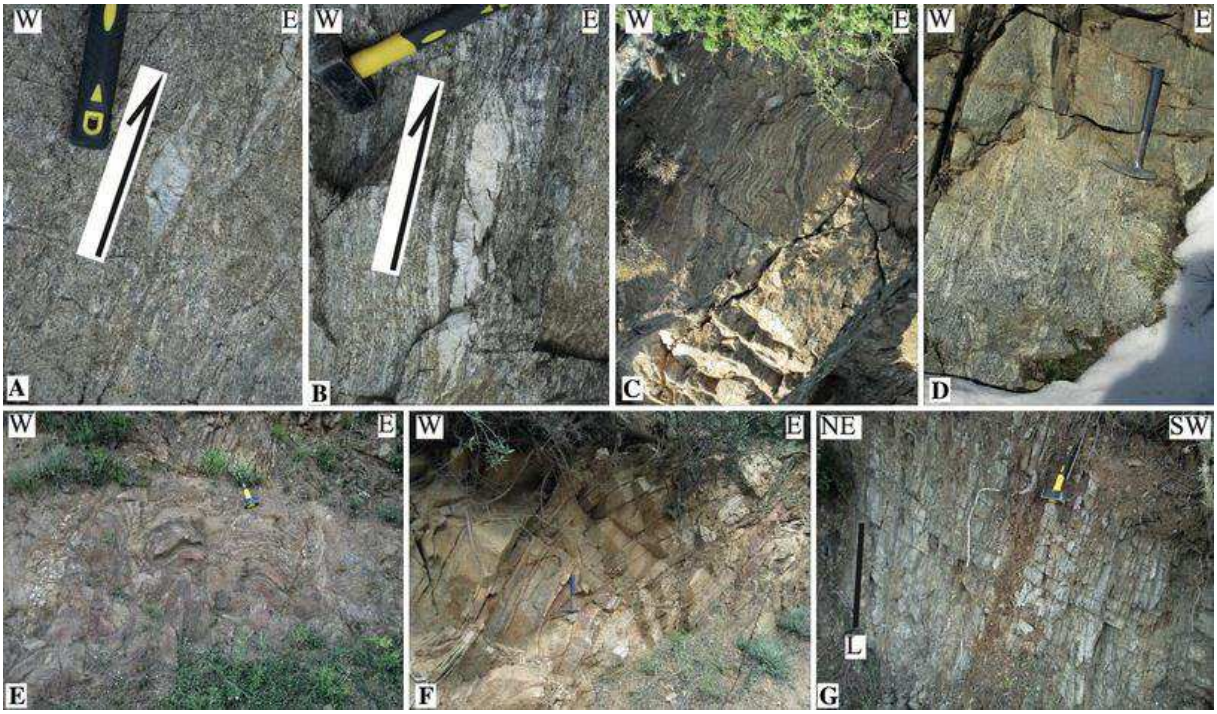

Fig. 12. Field-scale pictures from the Belgodère and Topiti areas. A: sigma-type K-feldspar megacryst showing a top-to-the-E sense of shear (Asco); B: sigmoidal leucosome in metatextite with top-to-the-E shearing (Asco); C: folded metatexite with westward vergence in the overturned limb of the antiform near East of Vallica; D: pervasively foliated and folded metatexite near Vallica; E: E-verging folds in non-melted restitic paragneiss, W of Asco; F: m-scale boudin in the leptynite-amphibolite series near Belgodère; G: amphibolite showing subvertical foliation and down dip mineral lineation in the Topiti area.

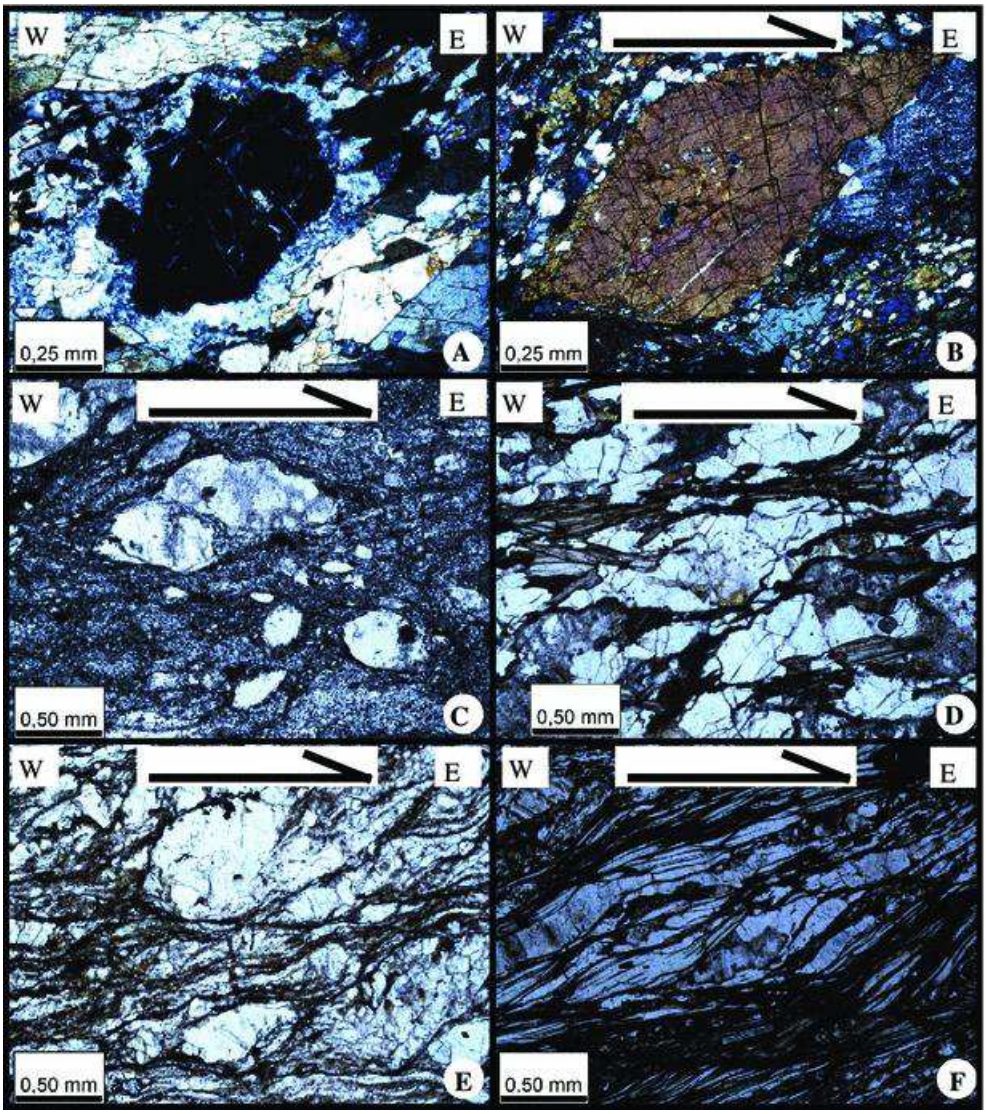

Fig. 13. Microscope-scale pictures from the Belgodère area. A: Plagioclase-quartz symplectitic rim around garnet indicating retrogression of an early eclogitic metamorphism in garnet amphibolite from Vallica; B: top-to-the-E asymmetry in amphibole from Belgodère metagabbro; C: top-to-the-E sheared K-feldspar clast in metaconglomerate, N. of Vallica; D: top-to-the-E sigmoidal quartz-feldspar aggregate paragneiss, Asco valley; E: top-to-the E shear bands with biotite coating along shear surfaces, Asco valley; F: top-to-the-East sigmoidal muscovite in Vallica micaschist.

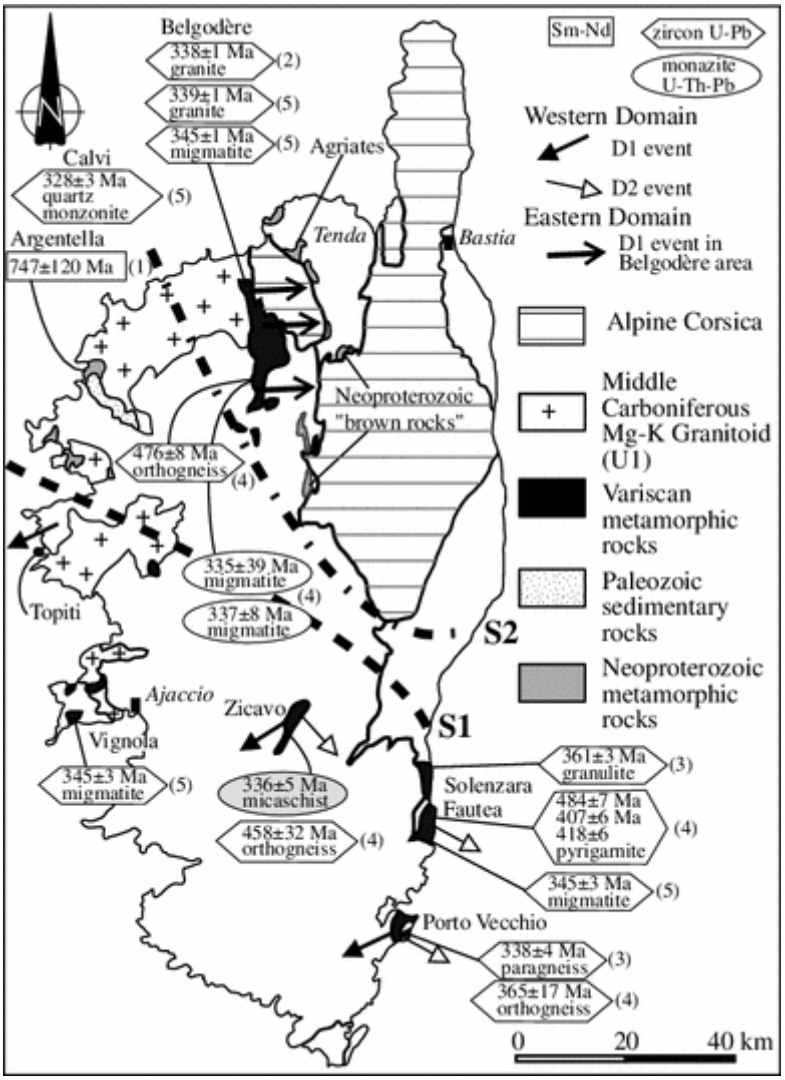

Fig. 14. Synthetic map location of the available geochronological constraints. 1: Rossi et al., 1995; 2: Paquette et al., 2003; 3: Giacomini et al., 2008; 4: Rossi et al., 2009; 5: Li et al. in review. The grey ellipse corresponds to the new U-Th-Pb age given in this paper. The two S1 and S2 possible sutures, and the kinematics associated with the deformation events described in the text.

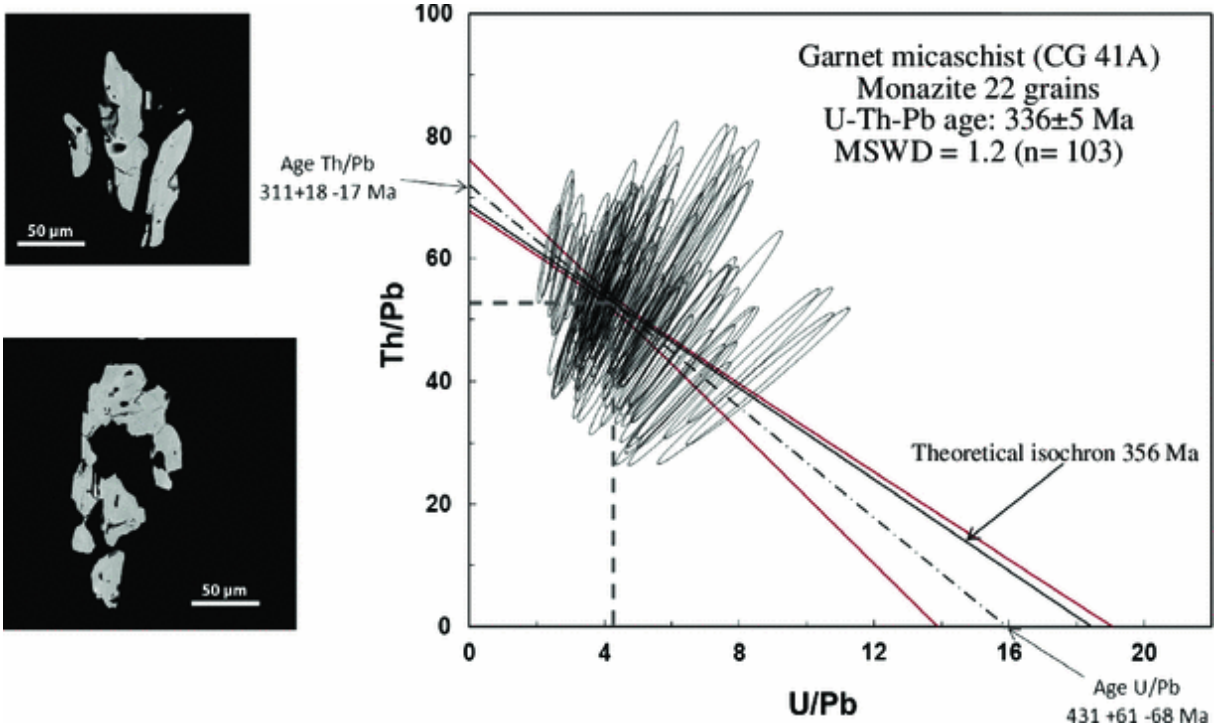

Fig. 15. Monazite U-Th-Pb ages of biotite-garnet micaschist from the Zicavo area, and SEM images representative of dated grains.

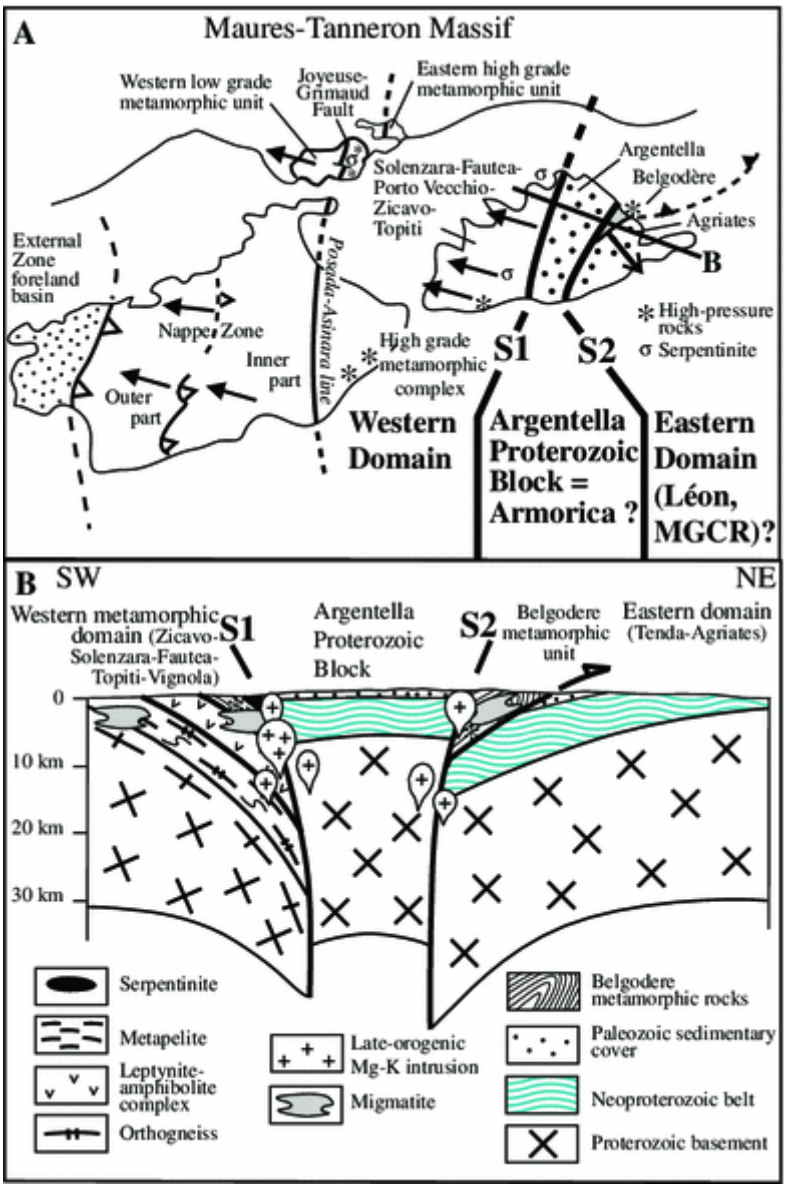

Fig. 16. A: Structural map of the Corsica-Sardinia-Maures Variscan massif showing the possible correlations between the three massifs, and occurrences of high-pressure metamorphic rocks and serpentinites. Arrows indicate the main deformation phase in the Western and Eastern Domains. B: Schematic crustal-scale cross section of Variscan Corsica showing the Western and Eastern domains, the intermediate Argentella Proterozoic Block bounded by the two S1 and S2 sutures with opposite vergence. The Western and Eastern Domains are tentatively correlated with the Armorica, and Mid German Crystalline Rise (MGCR)-Léon Block, respectively.